

Gonzalo Almanza Álvarez

Microfluidics Mixing using Surface Acoustic Waves (SAW)

Master's thesis in Supervisor: Carlos A. Dorao
June 2019

Acknowledgements

First of all, I want to thank to my supervisor Carlos Alberto Dorao, for giving me the chance of working in this fascinating project and for helping me in each step of its development.

Thanks to Jonas M. Ribe for teaching me every aspects of the process and for being always a help and support.

I also want to thank to my college Diego Sanchez Saldaña, who I have been working with and helping each other since we started the project, for always being free to discuss.

Finally, I want to thank to all Nanolab users and engineers for their support in the fabrication process.

Abstract

Nanoparticles detection by sensors uses samples quantities in the order of $10^{-9} - 10^{-18}$ L. Due to its inherent low Reynolds numbers, laminar flow is dominant in microfluidics, what leads to no fluid mixing and the need of an external force for achieving this. Mixing in these devices is necessary for enhance the contact between the sensor and the analyte, in order to improve the sensing efficiency.

In this project, mixing enhancement of microfluidics will be studied by the apply of Surface Acoustic Waves (SAW). When SAW are propagated through a substrate surface and get in contact with a fluid, they provoke a stirring on it and eventually, when the power is enough, they break the laminar flow and mix the fluid. For this goal, a microfluidic mixer will be fabricated, using a nano- and microfabrication method called “Photolithography”. This will be formed by a PDMS microchannel, for sample management, and an Interdigital Transducer (IDT), over a piezoelectric substrate, for the producing of SAW and fluid mixing.

During the first stage of the project, the device fabrication processes was developed and optimized. Then, these devices were tested using a syringe pump, a SAW generator, a microscope, different light wavelengths and a fluorescent dye. Mixing is studied using flow rates from 600 to 6000 μ L/h and power with a maximum of 2,57W, which is limited by bubbles appearance inside the microchannel.

High efficiency mixing was achieved for flow rates from 600 to 1000 μ L/h, with future expectative of even higher flow rates mixing. Using a smaller microchannel that the ones found in the literature, we got results comparable to recent publications. Mixing results were compared in function of the distance between the IDT and the microchannel, so we could check that the closer the IDT, the higher the mixing. Related to the use of a Single IDT or two IDTs (Dual IDT), it was found that Dual IDT mixing is higher than Single IDT's, however this has a power limitation. Testing of different IDT designs was performed.

Contents

Acknowledgements	<i>i</i>
Abstract	<i>ii</i>
Contents	<i>iii</i>
List of Figures	<i>v</i>
List of tables	<i>vii</i>
1. Introduction	<i>1</i>
1.1. Motivation:.....	<i>1</i>
1.2. Goal and objectives:	<i>2</i>
1.3. Scope of the project:.....	<i>2</i>
2. Background	<i>3</i>
2.1. Microfluidics.....	<i>3</i>
2.2. Surface Acoustic Waves (SAW).....	<i>4</i>
2.3. State of the art:	<i>5</i>
2.4. Photolithography:.....	<i>9</i>
2.4.1. Soft lithography:	<i>13</i>
3. Fabrication	<i>14</i>
3.1. Microchannel:.....	<i>14</i>
3.2. IDTs:.....	<i>16</i>
3.3. Microchannel + IDT integration.....	<i>19</i>
4. Experimental Facility and Procedures	<i>21</i>
4.1. Experimental setup.....	<i>21</i>
4.2. Experimental procedures	<i>22</i>
5. Results	<i>24</i>
5.1. Evaluation of the operational conditions	<i>24</i>
5.1.1. Diffusion.....	<i>24</i>
5.1.2. Occurrence of bubbles	<i>27</i>
5.1.3. Dual IDT high power limitation	<i>28</i>
5.2. 80 MHz mixer:	<i>29</i>
5.2.1. Single IDT performance:	<i>29</i>
5.2.2. Dual IDT performance:.....	<i>41</i>
5.3. Other designs mixers	<i>43</i>
5.3.1. 120MHz mixer.....	<i>43</i>
5.3.2. 40MHz mixer.....	<i>44</i>
5.4. Analysis of mixing	<i>45</i>
5.4.1. Single IDT	<i>49</i>
5.4.2. Dual IDT.....	<i>54</i>

6. Conclusions	57
Appendix 1: Fabrication concepts.....	58
Appendix 2: Fabrication materials	61
Appendix 3: Microchannel fabrication process comparison	67
References.....	69

List of Figures

Figure 1: IDT parameters[16].....	5
Figure 2: Tesla’s electrical condenser design. [20]	5
Figure 3: White and Voltmer’s IDT. [12].....	6
Figure 4: Trung-Dung et al. Parallel IDT vs.Focused-IDT [27]	7
Figure 5: Single IDT design vs. Dual IDT design [29]	8
Figure 6: Microchannel size comparison between recent publications	9
Figure 7: Spin coating.....	10
Figure 8: Soft baking	10
Figure 9: Exposure representation	11
Figure 10: Positive vs. Negative photoresist.	11
Figure 11: Post-exposure baking representation.	12
Figure 12: Development representation of a negative photoresist.	12
Figure 13: PDMS soft lithography process representation.....	13
Figure 14: Microchannel design	14
Figure 15: Dual 80MHz IDT design.....	16
Figure 16: IDT’s features comparison.....	16
Figure 17: IDT and microchannel before plasma bonding.....	19
Figure 18: Microchannel + IDT after plasma bonding.....	20
Figure 19: Device bonded to SAW generator connection platform	20
Figure 20: Lab setup	21
Figure 21: Sample prepared for experiments	22
Figure 22: Flow from both inlets joining in microchannel.....	23
Figure 23: Flow 50/50 in the inlet: Sulforhodamine + water / water	23
Figure 24: Diffusion comparison: Péclet numbers around 1000 vs. Péclet numbers over 10000	25
Figure 25: Comparison of diffusion with different concentrations	26
Figure 26: Bubble appearing inside the microchannel.	27
Figure 27: Broken sample after overpassing power limit.....	28
Figure 28: Microchannel and both IDTs. Microscope + regular light.....	29
Figure 29: Mixing of 400 μ L/h using violet light: a) 0W; b) 500mW; c) 1W; d) 1,5W 30	
Figure 30: Mixing of 600 μ L/h using violet light: a) 0W; b) 500mW; c) 1W; d) 1,5W; e) 2W	31
Figure 31: Mixing of 800 μ L/h using violet light: a) 0W; b) 1W; c) 1,5W; d) 2W	32
Figure 32: Mixing of 1000 μ L/h using violet light: a) 0W; b)1W; c)1,5W; d)2W	33
Figure 33: Mixing at maximum power, 2,57W for high flow rates, using violet light: a) 1500 μ L/h; b)2000 μ L/h; c)6000 μ L/h	34
Figure 34: Image comparison for 1000 μ L/h and 2W: a) Violet light; b) Green light....	35
Figure 35: Mixing comparison of 600 μ L/h. Violet light vs. Green light: a) 1W; b) 1,5W	36
Figure 36: Mixing comparison of 800 μ L/h. Violet light vs. Green light: a) 1W; b) 2W37	
Figure 37: Mixing comparison of 1000 μ L/h. Violet light vs. Green light: a) 1W; b) 2W	38
Figure 38: Mixing comparison of high flow rates at maximum power, 2,57W. Violet light vs. Green light	39
Figure 39: Comparison performance IDT1 vs. IDT2	40
Figure 40: Single IDT vs Dual IDT mixing of 600 μ L/h comparison.: a) 1W and 0W; b) 1W and 500mW.....	42

Figure 41: Single IDT vs Dual IDT mixing of 800 μ L/h comparison.: a) 1W and 0W; b) 1W and 700mW	42
Figure 42: Mixing comparison of 600 μ L/h using a 120MHz mixer: a)0W; b)2W	43
Figure 43: Mixing comparison of 800 μ L/h using a 120MHz mixer: a)0W; b)2W	44
Figure 44: Microchannel full with water. Regular light	45
Figure 45: No mixing image used as a reference in Matlab	46
Figure 46: Different mixing images in grey, made by Matlab	46
Figure 47: 600 μ L/h mixing curves using Violet light	47
Figure 48: 600 μ L/h mixing curves using Green light	47
Figure 49: 400 μ L/h mixing curves, using Violet light	49
Figure 50: 800 μ L/h mixing curves, using Violet light	50
Figure 51: 800 μ L/h mixing curves, using Green light	50
Figure 52: 1000 μ L/h mixing curves, using Violet light	51
Figure 53: 1000 μ L/h mixing curves, using Green light	51
Figure 54: 2000 mixing curves	52
Figure 55: Mixing comparison related to distance to the fluid.....	53
Figure 56: Mixing curves Singe IDT vs. Dual IDT for 600 μ L/h	54
Figure 57: Mixing curves Single IDT vs. Dual IDT performance for 800 μ L/h.....	55
Figure 58: Mixing curve of 800 μ L/h, comparison with maximum power for this flow rate	56
Figure 59: Lift-off representation process.	59
Figure 60: Comparison of gold deposition in a substrate with a photoresist without image reversal vs. AZ5214E	59
Figure 61: MLA 150 [45]	62
Figure 62: Plasma cleaner.....	63
Figure 63: Spin coater.....	64
Figure 64: AJA sputter and evaporator.....	64
Figure 65: MA6 [45].....	65
Figure 66: Wire bonder [45]	66
Figure 67: SU8 microchannel pattern features	67
Figure 68: mr-DWL microchannel pattern features	68

List of tables

Table 1: Flow conditions, Reynolds and Péclet numbers.....	25
Table 2: Light source parameters comparison.....	35
Table 3: Microchannel fabrication process comparison.....	67

1. Introduction

1.1. Motivation:

Exosomes are extracellular vesicles that can be found in all human fluids including blood and urine. First found in mammalian blood cell, they are secreted by a multitude of different kind of cells and are 40 to 100 nm big. [1] At first, scientists thought that they were waste products. [2] However, after that, was discovered that they play an important role in different cell functions, as cell-to-cell communication, antigen presentation and transfer of oncogenic proteins. [3] Exosomes contain molecular components from their cells of origin, so after years of research, scientists are able to determinate the nature of these cells. [1] Thank to this, exosomes can be used for medical studies, i.e. early cancer detection, as recently has been discovered, that cancer-derived exosomes contain proteins related to tumour progression. [3]

Due to its tiny size, detection and isolation of exosomes have been challenging for scientists. Detection is done using different kinds of sensors, however, in most of them the sample is managed using microchannels and what it is called microfluidics.[4] Due to its laminar flow inside the microchannel, inherent in microfluidics, just a small part of the sample gets in contact with the sensor, what leads to low efficiencies. In order to improve the efficiency of these sensors, it is necessary to enhance the mixing in the channel with some active or passive devices. One particular concept is the Surface Acoustic Waves (SAW) for microfluidic mixing. This concept has the advantages of being not aggressive with the sample, as other methods, and as it has not moving parts, it is cheaper and more reliable.[5][6]

Mixers that use SAW for fluid stirring have shown that have a high efficiency, despite of this, its mixing capacity is still limited, during this project we will study how to improve this.[5] We want to fabricate a prototype of acoustofluidic mixer that, using Surface Acoustic Waves (SAW), produced by an Interdigital Transducer (IDT), triggers mixing of fluids inside a microchannel.

1.2. Goal and objectives:

The goal of this project is to advance in the development of enhance mixing devices at low Reynolds numbers.

The main objective in this work is to study the mixing properties of a SAW mixer integrated with a microchannel. In particular, the objective is to identify the required power input in order to achieve high efficiency mixing in a Y microchannel configuration for different flow rates as well as compare different mixing scenarios and determinate the optimum one.

The main tasks in the work have been:

- Fabrication of a prototype of "Acoustofluidic mixer" with two IDTs
- Fabrication of acoustofluidic mixers with different designs of IDTs
- Comparison of the different designs
- Comparison between mixing performance of a Single IDT and Dual IDT

1.3. Scope of the project:

This work has been focused on Y-shaped microchannel with two inlets, that join and become a single channel, with a length of 7mm from the joint, a width of 100 μ m and a height of 56 μ m. The flow rate considered were in the range 600 – 6000 μ L/h. The IDTs have frequencies of 40, 80 and 120 MHz, with fingers of 8,6, 12,5 and 25 μ m wide, and finger spacing equal to the width. The electrodes of the IDTs are made by a 80nm gold layer. Photolithography, using a tool called MLA, was the fabrication process for this device.

A syringe pump is used for flowing two different fluids into the microchannel and the IDT, connected to a SAW generator, for mixing both fluids.

2. Background

2.1. Microfluidics

Microfluidics are defined as the science and technology of systems that manipulates amounts of fluids in a range between $10^{-9} - 10^{-18}$ L, using microchannels [OandFMF]

The first applications of microfluidics were in analysis, thanks to its capabilities, as using very small quantities of samples and reagents, and to carry out separations and detections with high resolution and sensitivity; low cost; short times for analysis; and small footprints for the analytical devices [7 OandFMF]

The ratio of physical phenomena, that occurs in microfluidics, is expressed by the dimensionless numbers that defines a fluidic system. [8] For our case we will focus on Reynold's and Péclet numbers:

Reynold's numbers are the most often mentioned rely with microfluidics, however, it might be the less interesting number in this field: in all microfluidic devices, Reynold's numbers are so small that inertial effects are irrelevant. [Microfluidics: Fluid physics at the nanoliter scale] It represents the ratio of the fluid momentum to the viscous friction force, and its expression is $Re = VL_h/\nu$, where V is the average flow velocity, L_h is the hydraulic diameter and ν is the kinematic viscosity. [9] Turbulent flow happens where Reynolds numbers are high, however, with low Reynolds numbers, viscous forces are dominants. This leads to pure laminar flow, where turbulences are not possible and mixing times are determined by diffusion.[10]

Péclet number expresses the relative importance of convection to diffusion [Microfluidics: Fluid physics at the nanoliter scale] and is expressed as $Pe = VL/D$, where V is again the average flow velocity, L is the length of the mixing path and D is the diffusion coefficient. [9] If the Pe is lower than 1000 the flow is considered to be diffusive dominant.

Microfluidics are used in exosomes detection, as microchannels are the way to make the sample interact with the analyte. As a consequence of poor mixing, the number of interactions between the analyte and the sensor is low, so are the chances of binding events, giving poor results. The way of improving these results is achieving a bigger amount of fluid getting in contact with the sensors, for what is necessary a higher level of mixture. Since recently microfluidic systems have become so popular because

their application in “labs-on-a-chip”, all scientists and engineers have found in getting an efficient mix a big issue. Both low Reynolds and high Péclet numbers, combined in microfluidics, make these systems extremely resistant to mixing. [5]

To solve this issue, many mixers have been proposed during the last years, we can divide them in two kinds: active mixers and passive mixers. Passive mixers are those in which mixing depends on the microchannel design. In passive mixers, diffusion mixing is enhanced increasing the contact area using different microchannel designs, what has been proved that gets high throughputs; or increasing contact time, what normally leads to inefficient mixing results and also needs longer microchannels. Active mixers performance is produced by stirring and agitating of the fluid with the application of an external energy force, produced by acoustic/ultrasonic, dielectrophoretic, electrokinetic time-pulse, pressure perturbation, electrohydrodynamic, magnetic or thermal techniques. [6]

In this project, we will try to develop an active mixer, that uses Surface Acoustic Waves (SAW) for mixing of fluids in a microchannel.

2.2. Surface Acoustic Waves (SAW)

Surface Acoustic Waves can be generated at the free surface of an elastic solid.[Colin Camp] They were first discovered by Lord Rayleigh in 1885, he described its properties and mode of propagation; they were also named after him as Rayleigh Waves. [11] Waves propagated along] In 1965, with the invention of the *interdigital transducer* (IDT) by White and Voltmer, SAW technology was first applied to electronics.[12] This invention supposed the most efficient technique for generation and detection of SAW in a piezoelectric substrate [13] But it wasn't until the beginning of the 1980's, that electro-acoustic devices started to gain importance for its technical application in electronics, electronic data processing and high-frequency technology. [14]

As we explained above, SAW are produced by IDTs; these are directly deposited in the substrate's surface and formed by embedded electron pairs. The application of a high frequency voltage through the IDT leads to a deformation of the surface, what creates the SAW, with a frequency defined by the IDT finger spacing +

finger width, d , and the substrate acoustic velocity, C_{SAW} , given by the expression: $f = C_{SAW} / 2d$. [10][15]

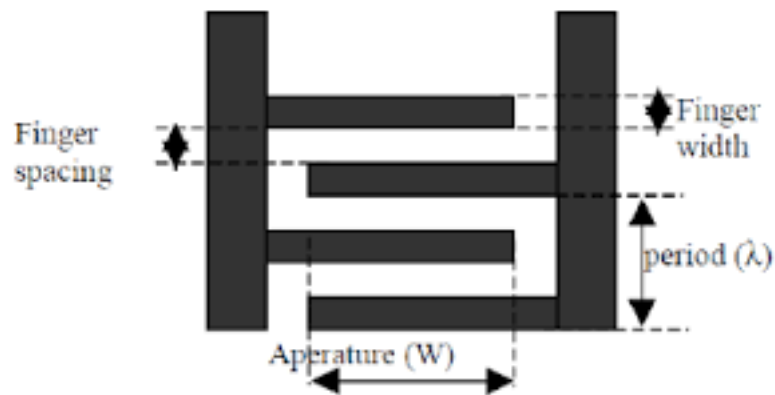


Figure 1: IDT parameters[16]

This phenomenon has allowed the development of different devices and systems for consumer, commercial and military applications [17] and we could say that many of these SAW devices overcome those based on other competing technologies. [18]

2.3. State of the art:

Perhaps, the first example of an interdigital electrode was design by Nicola Tesla in 1891, he called it “electrical condenser”. In this device, the capacitance increased linearly with the number of plates, what in modern IDT would be the fingers. [19]

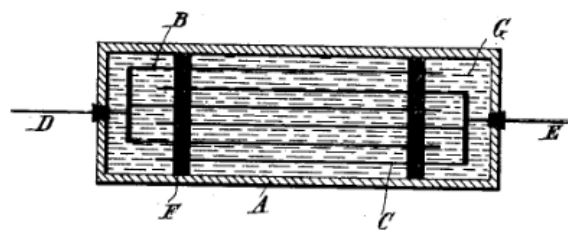


Figure 2: Tesla's electrical condenser design. [20]

In Figure 2we can see the design made by Tesla for its electrical condenser.

In 1965, as it is mentioned previously, White and Voltmer produce the first SAW using an IDT, by two electrodes made by a 1000 Å thin Aluminium layer vacuum-deposited over a quartz bar. The biggest disadvantage of this device was the difficulty for the piezoelectric orientation of the materials. [12]

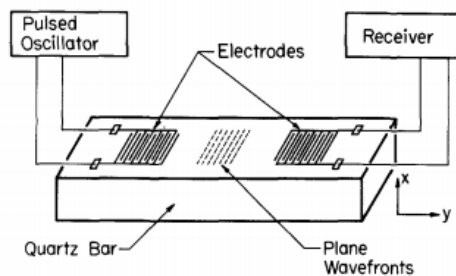


Figure 3: White and Voltmer's IDT. [12]

This investigation was supported by the US Army and, until the 1980's, this technology was used just for military purposes. Later, it began to be used for other applications as electronics and communications and in the last decades it was introduced in other fields like chemical sensing or biomedical applications. [19]

In the decade of 1980s, the first articles about the applications of SAW devices as chemical sensors appeared. Previous studies, defended that SAW could only operate with gas-phase fluids, based on experience with bulk wave sensors. [21][22] However, in later researches, the idea of a liquid-phase SAW-based chemical sensor was defined. [23] In 1987, a study made by Gary S. Calabrese, Hank Wohltjen and Manas K. Roy, firstly explored the use of SAW devices, with frequencies of 10, 30,31 and 50 MHz in quartz substrates as liquid-phase chemical sensors.[24]

A decade later, in 1998, SAW technology was, for first time, applied for microfluidics mixing at low Reinold's numbers by A.Yotsumoto, R.Nakamura, S.Shoji, T.Wada. [25] In this work, they develop an integrated mixing/reaction micro flow cell. In order of reduce the analyzing time, they combined macro pores Si fabricated and SAW for stirring, for producing flow mixing. They fabricated a SAW device, with 400µm electrode pitch and finger width of 20µm, in a $LiNbO_3$ substrate, with a frequency of 10MHz.

In 2006, Wei-Kuo Tseng, Jr-Lung Lin, et al. developed the first active micro-mixer using SAW.[26] In this work, they fabricated PDMS microchannels, for fluidic handling, with a width of $200\mu\text{m}$. Over a single-side polished Y-cut 128°LiNbO_3 substrate, the IDT was fabricated, with $0,15\mu\text{m}$ of Aluminium and a frequency of 9,6 MHz. Applying SAW in both, parallel and transversal, directions, as different experiments, they achieved mixing.

In 2010, Trung-Dung Luong, Vinh-Nguyen Phan, et al. compared parallel electrodes with focused electrodes, that produced Focused-SAW. They determined that focusing types gave a better mixing efficiency. The microchannel has a width of $240\mu\text{m}$. [27] Following this experience, in 2011, Q.Zeng, F.Guo, et al. achieved milliseconds mixing using F-SAW, with a resonance frequency of 19,2 MHz in a distance of 1mm. [28]

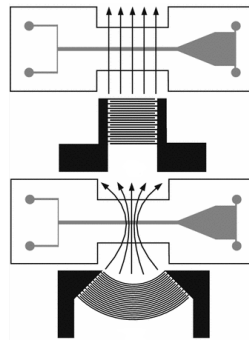


Figure 4: Trung-Dung et al. Parallel IDT vs.Focused-IDT [27]

In 2013, Myeong Chan Jo and Rasim Guldiken used two IDTs, dual SAW, one from each side of the microchannel, of $150\mu\text{m}$ width, doing a comparison of this vs. only one IDT. They could determine that dual IDT design increased mixing compared to single IDT design. [29]

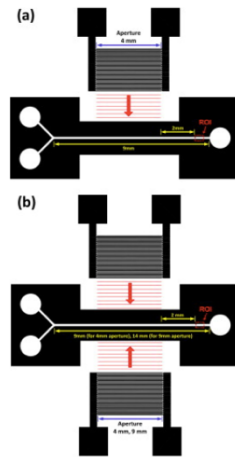


Figure 5: Single IDT design vs. Dual IDT design [29]

Another innovation in this field was developed in 2017 by Jeonghun Nam and Chae Seung Lim. They fabricated a three-dimensional dual SAW device for microfluidic mixing. Using a dual-IDT design, one IDT located in top, and another in the bottom of the substrate, they achieved around 100% mixing at 50 μ L/min and \geq 14 V. Microchannel used has a 400 μ m of width.[30]

Lately Husman Ahmed, Jinsoo Park et al.,(2019) have shown that it is possible to achieve complete mixing, of 100%, of 50 μ l/min of fluid, integrating an straight IDT with a $LiNbO_3$ substrate, beneath a PDMS microchannel, applying a high voltage of 140MHz. [31]

In summary, the use of SAW for microfluidic mixing has been studied mostly in the past decade, and in particular it has been applied for mixing in microchannels with a width over 150 μ L/h. However its use in channels below that size has not been reported. For our study we will use a 100 μ L/h wide microchannel.

In Figure 6 a microchannel size comparison between recent publications is shown:

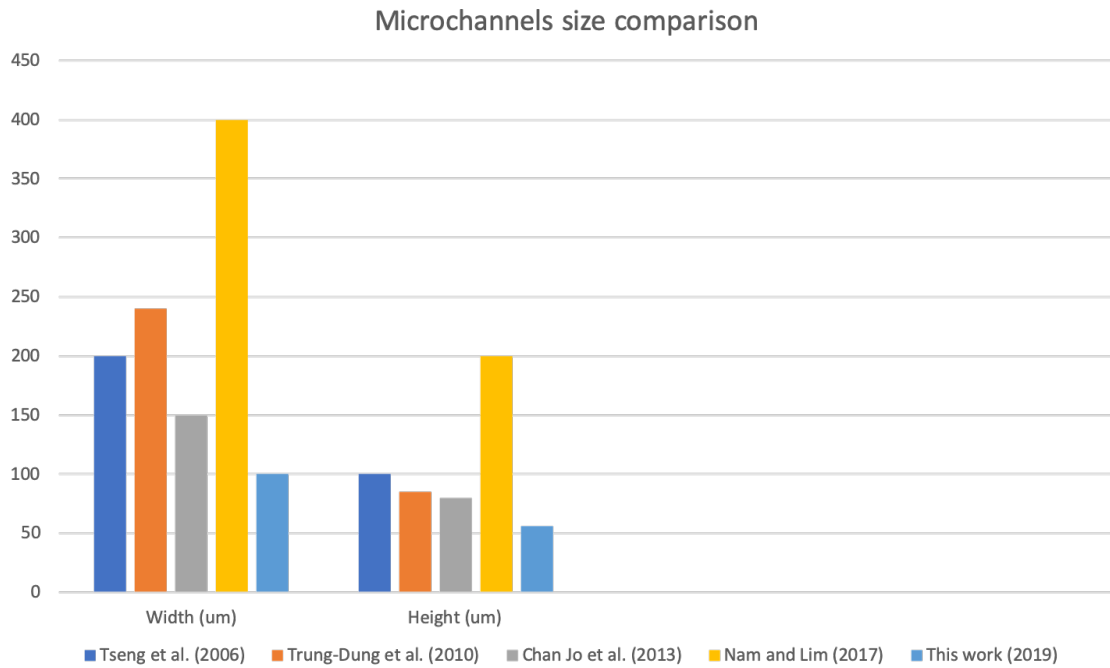


Figure 6: Microchannel size comparison between recent publications

2.4. Photolithography:

All produced devices discussed in the previous section have been based on a fabrication process, called “photolithography”.

Photolithography, is a process used in micro- and nanofabrication to transfer a pattern from a mask to a thin film of “photoresist”, a light sensitive chemical. Photolithography development started in earlies 1952 to 1958, with Jay Lathrop, an American PhD in physics. It became critical in the first efforts to produce semiconductor ICs, for the U.S. Department of Defense, on a project for develop microminiaturized, transistorized hybrid integrated circuits for radio proximity fuses. [32] Since its invention in 1959, it is the most successful technology in microfabrication and it has been the most used process in semiconductor industry. [33]

The process follows the next steps:

1) Sample cleaning:

Substrate cleaning is the first part of the process, it is necessary to eliminate all the organic material in the surface, before coating the photoresist, to make sure this material don't ruin it.

2) Dehydration bake:

A baking is made before the spin coating in order to eliminate all the humidity that could be in the substrate surface, improving this way the photoresist adhesion.

3) Spin coating:

A film of photoresist is placed in the surface of a properly cleaned substrate, using a spin coater. The spin coater allows us to obtain the thickness wanted for the photoresist and also distribute it homogeneously over the wafer.

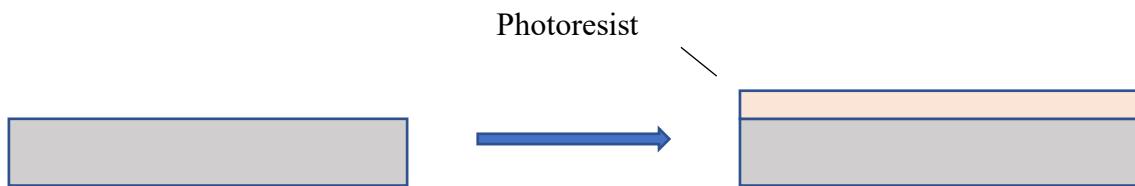


Figure 7: Spin coating

4) Soft baking:

After the layer of photoresist is applied, it still contains up to 15% of solvent and may contain built-in stresses, therefore, it is necessary to do a pre-bake to dry the resist film and densify the layer, making it more resistant. [34] This step is important, because if this is not correctly done, it may affect to the structural properties and the light-sensitivity of the resist.

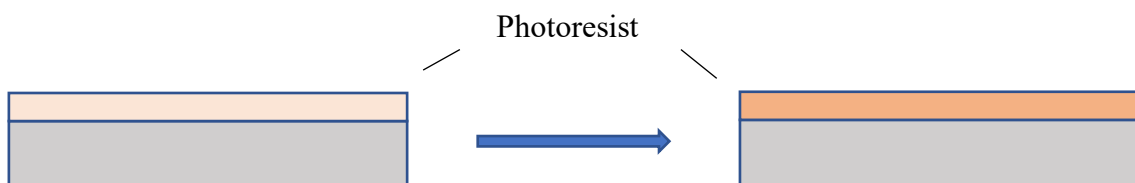


Figure 8: Soft baking

5) Exposure:

The sample is subjected to a UV light flood exposure. The emitted light intensity (W/cm^2) and the exposure time (seconds) gives the dose (J/cm^2) across the resist surface. This radiation triggers a reaction in the photoresist, affecting the solubility of the exposed areas in a certain solvent. [34]

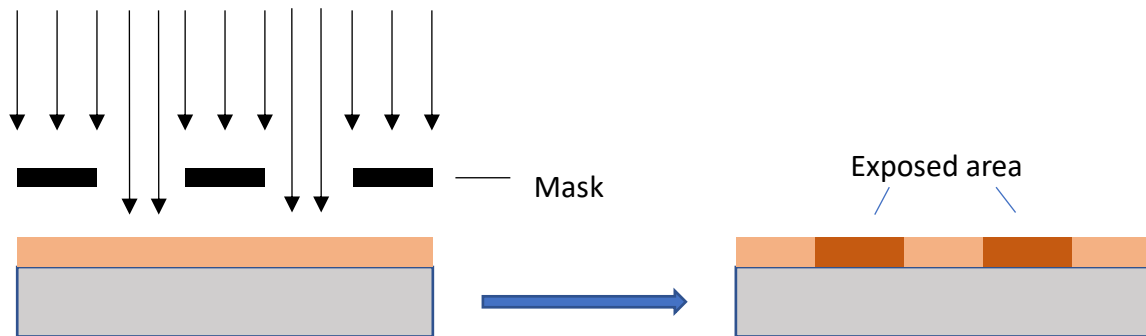


Figure 9: Exposure representation

It is necessary to explain the difference between a positive and a negative photoresist. In negative photoresist, the exposed areas become insoluble in a solvent, whereas the unexposed areas are dissolved during the development, so the final result of the process is the pattern exposed. On the other hand, a positive photoresist is one in which the radiation makes the exposed areas soluble during the development, while the unexposed areas remain after it. The final result is the negative design. [35] In Figure 10 it is represented the behaviour of them both when exposed.



Figure 10: Positive vs. Negative photoresist.

6) Post-exposure baking:

Depending on the resist a post-exposure bake (PEB) step might be required. A PEB completes the reactions started in the exposure, that might not be finished. It completes

the cross-linking, improves adhesion, reduces scumming and increases contrast and resist profile. [34] Figure 11 shows the resist before and after it.



Figure 11: Post-exposure baking representation.

7) Development:

Development is the part of the process where soluble areas of the photoresist are dissolved, turning the latent resist image, formed during exposure, into the structures desired. [34] In Figure 12 we can see the development process for a negative photoresist.

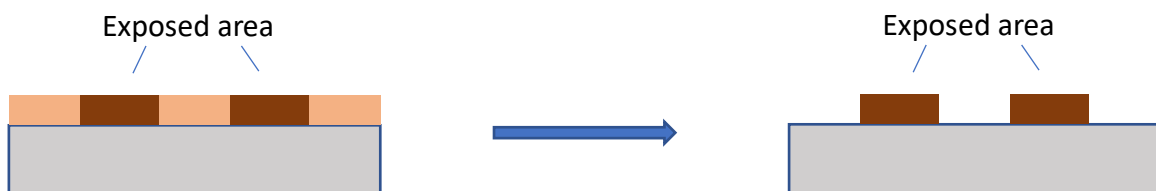


Figure 12: Development representation of a negative photoresist.

8) Hard bake (Optional)

After the development, depending of the resist and as an optional step, another baking is made in order to improve etch resistance or minimize outgassing. [36]

In the recent years, a new kind of tool called Maskless Aligner has been developed, where no mask is needed and the exposure is done directly using a laser. This is the tool mainly used for photolithography in this project. [Appendix 1]

2.4.1. Soft lithography:

Soft lithography is the process of replicating a structure in a soft polymer. In this type of lithography, light is not intervening, but the molds are typically made by photolithography. It is therefore an extension of photolithography and represents a possibility for rapid prototyping of various microscale and nanoscale structures and devices. [37] We used it in the fabrication of microchannels.

Polydimethylsiloxane (PDMS) is the most widely used polymer for soft lithography due to its strain and flow properties. It is transparent and non-flammable silicon-based polymer. [33] Once we have the pattern of the microchannel in the substrate, this is used as a moulding. It is covered with liquid PDMS and, after a baking where it gets the desire rigidity, the microchannels are ready to be peeled off from the sample.

When the PDMS is separated from the sample, the structure of the microchannel is already printed on it, obtaining its wanted shape.

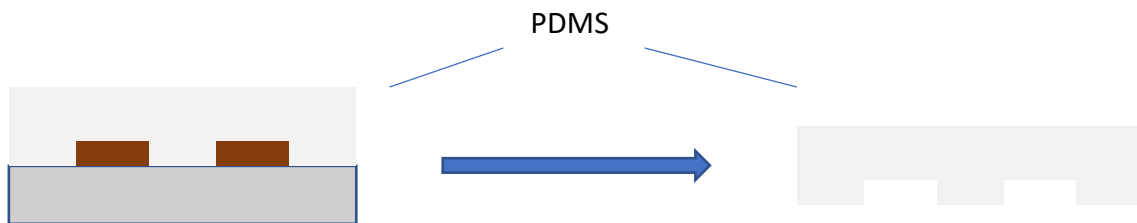


Figure 13: PDMS soft lithography process representation.

In Figure 13 is shown how would be the result of the PDMS microchannel structures after curing it and peel them off.

3. Fabrication

In this part, it will be described the parameters used in the device fabrication, explaining each process for the microchannels, the IDTs and the final assembly. The recipes used will be explained here, tools and materials used, are detailed in the Appendix 2.

3.1. Microchannel:

For the microchannels fabrication it is used a 2 inch Si wafer as substrate, SU-8 as photoresist and PDMS for the soft lithography. In the Specialization project we did a process comparison using two different photoresists and we determine SU-8 as the optimal [Appendix 3]. In Figure 14 is shown the design of the microchannel:

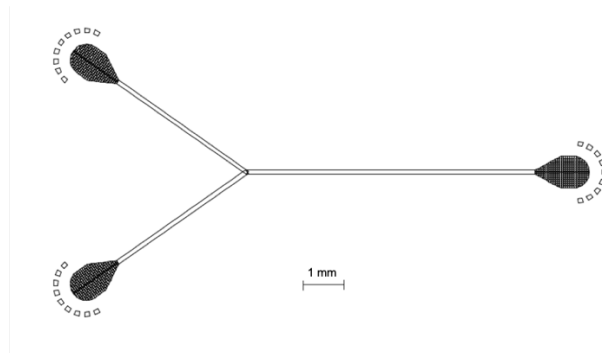


Figure 14: Microchannel design

Substrate cleaning:

We spill the sample first with acetone and, before it dries, with IPA. After this, we dry the substrate with N_2 .

Next to this, we use the Plasma cleaner to remove all the organic material that could remain in the substrate.

Parameters for plasma cleaner are O_2 , 50/50 for 5 minutes.

Spin coating:

For a thickness of 50 μ m, we introduce in the spin coater the next data:

Initial: 500rpm for 12s; Final: 3000rpm for 46s; Rampage: 250rpm

Soft bake:

After the spin coating, it is necessary to do the soft bake.

We bake the sample for 15min at 90°C.

Exposure:

Exposure is made using the MLA.

We use the 375nm wavelength laser with a dose of 2000 mJ/cm^2

Post-exposure Bake:

Once the exposure is completed, PEB is needed, its parameters are:

1min at 65°C + 4min at 95°C

Development:

We use the developer mr-Dev 600.

Development time: 5 minutes.

After the development we clean the sample with acetone, IPA and dry it with N_2 .

Soft Lithography

We cover the substrate with PDMS and we introduce it in the oven at 65°C for 2 hours for curing.

3.2. IDTs:

For IDT fabrication we use $LiNbO_3$ as substrate, AZ5214E is the photoresist chosen. This is a long and difficult process and, although we have been doing it for this whole year, many things can go wrong. This implies that $\frac{1}{2}$ of the IDTs that we fabricate are not valid and, even more challenging, is to get a sample with both IDTs operative. The most difficult to fabricate was the 120MHz one, due to the small size of its features.

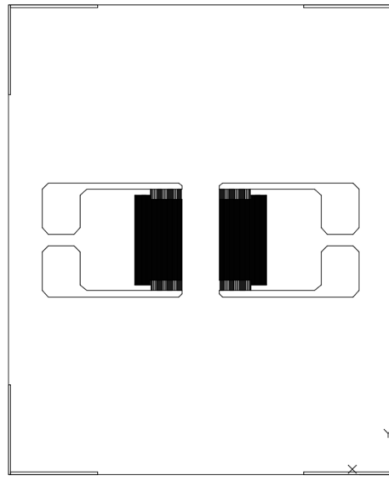


Figure 15: Dual 80MHz IDT design

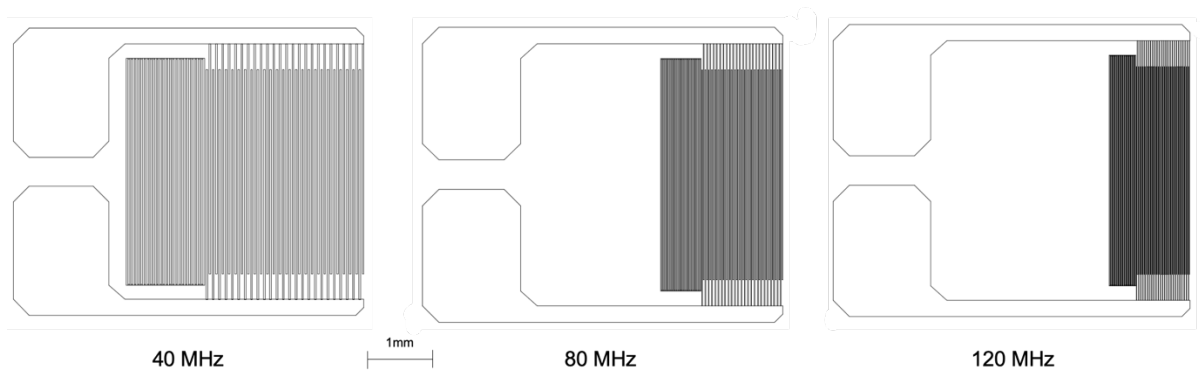


Figure 16: IDT's features comparison

Figure 15 shows the design of a Dual 80 MHz IDT used for fabrication. In Figure 16 we can see a feature comparison between the IDTs of the different designs.

Cleaning:

The substrate is spilled with Acetone, IPA and dried with N_2 .

Afterwards, it is cleaned with O_2 plasma 50/50 in the plasma cleaner for 5 minutes.

Dehydration bake:

After the cleaning, the sample is baked at 110°C for 5 minutes, to make sure that we eliminate all the humidity that could remain in the surface of the substrate before the spin coating.

Spin coating:

We want to obtain a photoresist layer thickness of $1,5\ \mu\text{m}$.

Spin parameters: 4000 rpm for 46 seconds, rampage of 4000 rpm.

Soft bake:

We bake it at 95°C for 90 seconds.

Exposure:

We use the laser of $405\ \mu\text{m}$ of the MLA.

Dose = $27\ \text{mJ}/\text{cm}^2$.

Image reversal bake [Appendix 1]:

When the pattern is exposed, it is time to do the image reversal, for what we do bake the sample at 113°C for 2 minutes.

The temperature of this baking is really important because it affects to the crosslinking, what determines the angle of the structures, guaranteeing the lift-off.

Flood exposure:

We use a Mask Aligner, MA6, to do a flood exposure to the sample of 200 mJ/cm^2 , this is made for making the non-exposed zones of the photoresist, soluble in the developer, while the exposed pattern remains.

Development:

For developing we use AZ726 MIF for 40s, last 10s stirring.

After development we clean the sample using ID and then dry it with N_2 .

Deposition:

We deposit 5nm of Ti with a rate of 5 \AA/s , for ensuring gold attaching to the substrate.

After the Ti, we deposit 80nm of Au with a rate of 5 \AA/s .

Lift-off [Appendix 1]:

Lift-off was made in a beaker with acetone, using an ultrasonic bath at room temperature for 1 minute.

Then, we try to remove the last gold particles that could remain in the surface using a pointed swab sodden in acetone.

3.3. Microchannel + IDT integration

First of all, we punched the inlets and the outlet of the microchannel, where the tubes will be placed for introducing and collect the fluids.

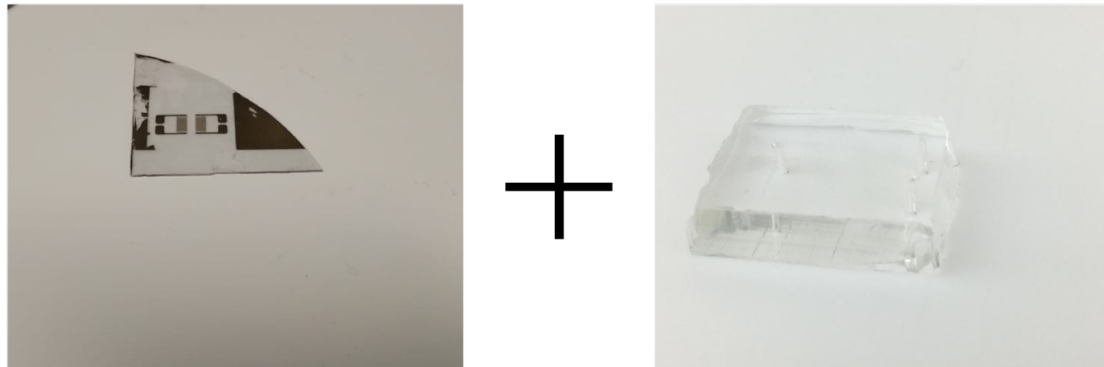


Figure 17: IDT and microchannel before plasma bonding

After this, the next step is to join the microchannel and the IDT, plasma bonding the PDMS microchannel to the IDT. For this, we surface activate the PDMS with the plasma cleaner [Appendix 1]. We introduce both IDT and PDMS microchannel in this tool and do a O_2 at 50% plasma treatment at 20% of power. Next, we spill some ethanol over the IDT for retarding the bonding, in order to get a proper alignment and we place the microchannel in the right position. Finally we bake the whole device for 15 minutes in the oven at 65°C for finishing the crosslinking. This is a really delicate process and there is no way you can ensure its working, many of the times the bond is weak, normally next to the inlets/outlet, so leaking occurs very often. The bigger issue here is that you can not unbind the microchannel, so if a leaking appears, you must fabricate a whole new sample.

Figure 18 is a picture of the device once the microchannel is plasma bonded to the IDT.

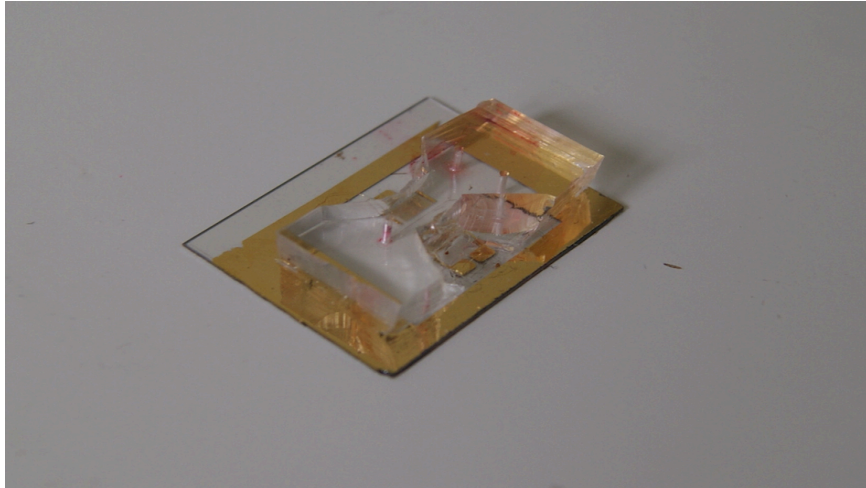


Figure 18: Microchannel + IDT after plasma bonding

Once the microchannel is attached to the substrate, we have to wire the sample to the platform that allows us to connect the whole device to the SAW generator. This process is made using a wire bonder, that through 25 μm gold wires, makes a connection between the IDT and the platform. This is a very difficult step, we normally spend several hours to make the connections. In Figure 19, in the centre of the picture, the gold wires can be seen.

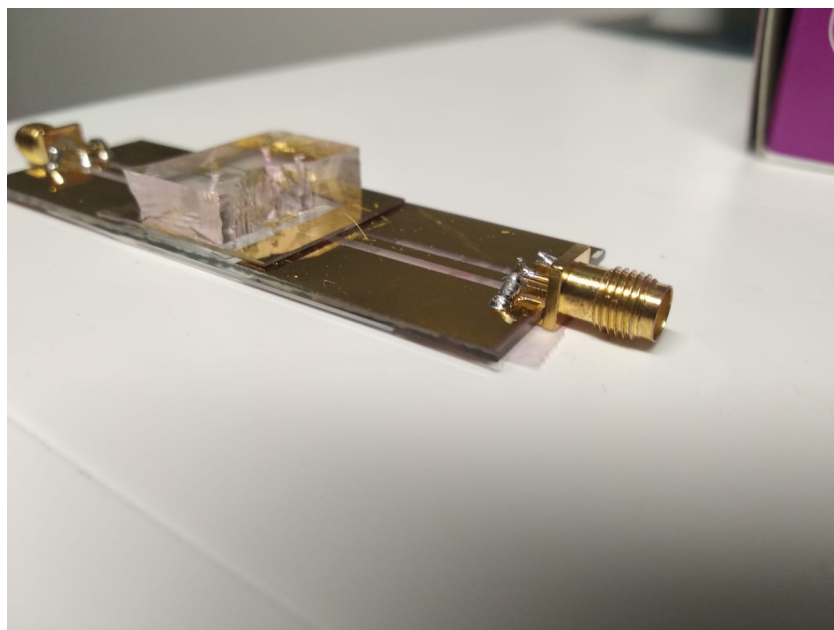


Figure 19: Device bonded to SAW generator connection platform

4. Experimental Facility and Procedures

In the experimental part, we want to test the devices that we fabricated and try to mix fluids inside the microchannel. We introduce two fluids through the microchannel inlets and using the IDTs, connected to a SAW generator, we produce Surface Acoustic Waves and try to break the laminar flow. The mixing is observed using an inverted microscope and illuminating it a light with specific wavelengths, or colours.

Notice that during the experiments, most of the samples get ruined, either because of a leaking or because of a crash due to high power. This means that the fabrication is always active, it is necessary to keep producing samples in order to be able to continue with the experiments. More than 10 sample were tested, during the first experiments, so we could learn how to deal with the problems and start obtaining results. After this, a bunch of around 10 more samples were used.

4.1. Experimental setup

The study of the microfluidic mixing was done in an experimental facility consisting in the elements shown in Figure 20.

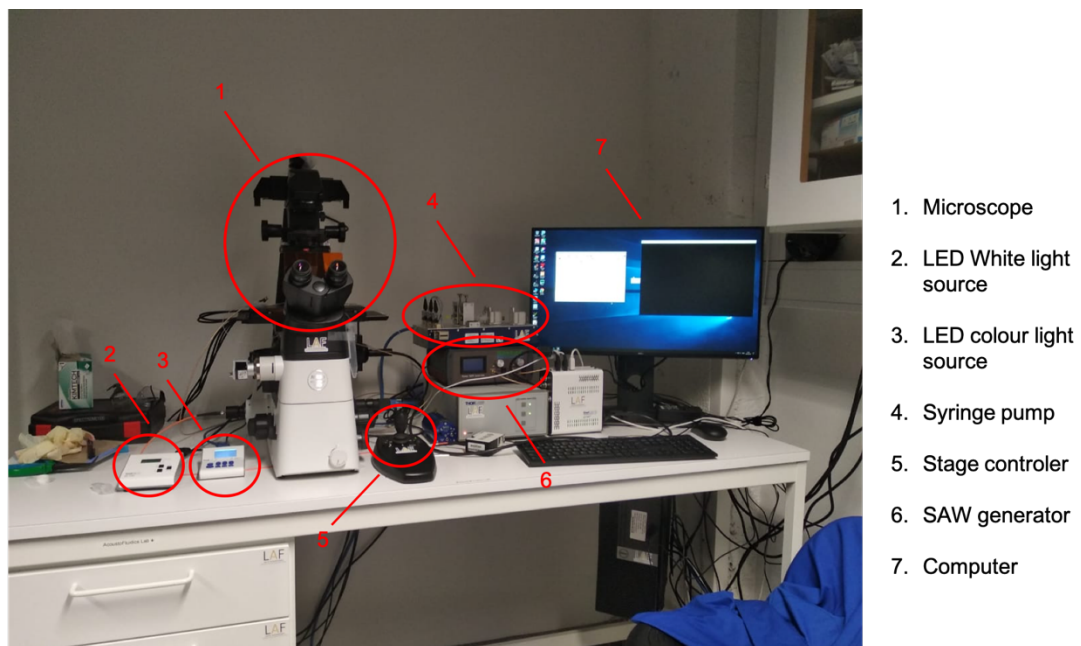


Figure 20: Lab setup

4.2. Experimental procedures

First of all, the sample is placed in the stage of the microscope and connected to the SAW generator by two cables, one at each side of the sample. In order to avoid the light diffraction by the $LiNbO_3$ and obtain a right focused image, we add another piece of $LiNbO_3$ underneath the sample.

For running the experiments, two fluids for mixing are needed. In order to be able to do a good comparison and quantify this mixing, a solution of a fluorescent dye [28][29], Sulforhodamine B in our case, and DI-water are used. The solution is 0,5% Sulforhodamine B + water. This percentage of solute is determined after a comparison of different solutions changing concentrations. Solutions over 0,5% contained particles that eventually would accumulate and obstruct the channel. Solutions below 0,5% were not as fluorescent as we would desire. Next to the microscope there is the syringe pump. Two syringes are put in this device, for controlling the flow introduced in the microchannel. One syringe is filled with water and the other one with the solution of Sulforhodamine B.

From these syringes, two tubes, one from each, are connected to the inlets of the microchannel. Another tube is connected to the outlet and led to a container, attached to one side of the microscope with tape, in order to collect the fluid once it passes through the microchannel. In Figure 21 is shown a picture of the mixer while an experiment was running.

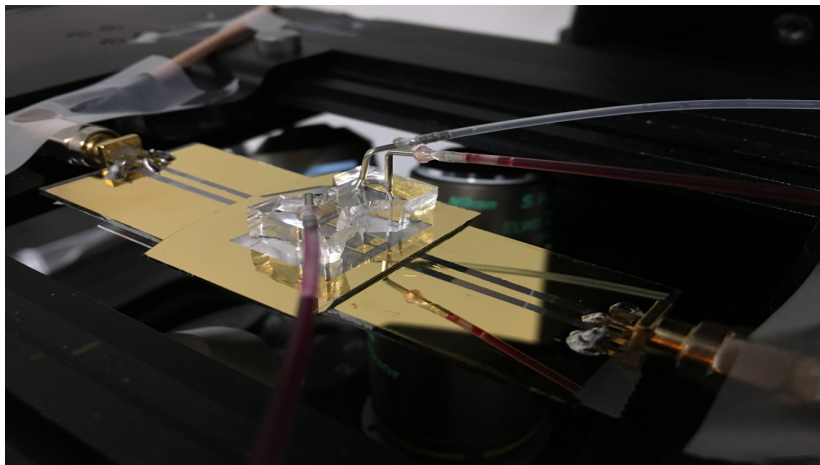


Figure 21: Sample prepared for experiments

With the syringe pump, controlled by a software, the desired flow is introduced in the microchannel, same for both syringes, and wait until it stabilizes 50/50.

Figure 22 shows the stream of both flows under regular light..

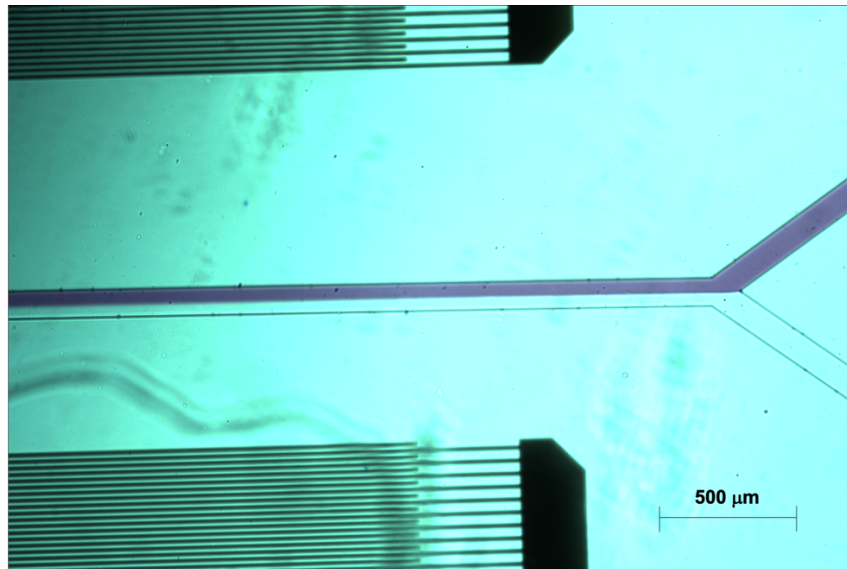


Figure 22: Flow from both inlets joining in microchannel

Figure 23 shows the stream of both flows under Violet light:

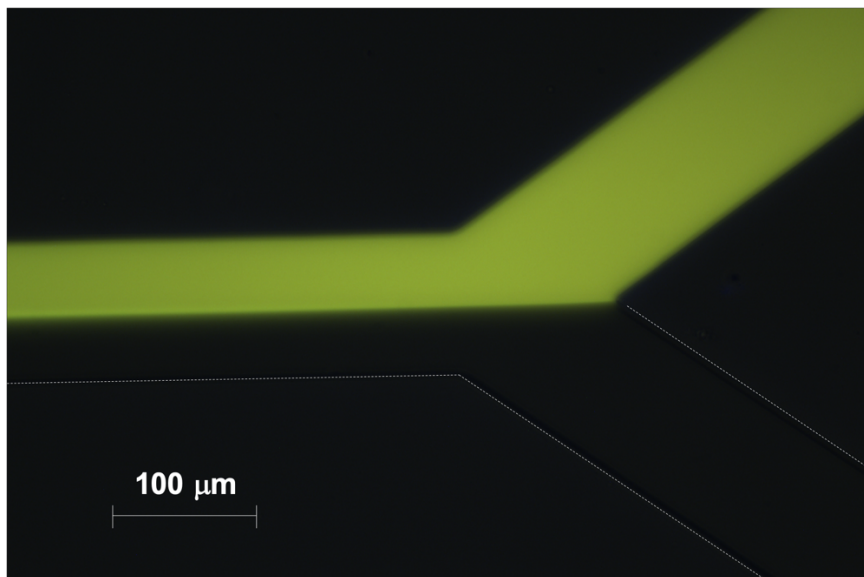


Figure 23: Flow 50/50 in the inlet: Sulforhodamine + water / water

5. Results

Results obtained testing the different devices, as experience from running the experiments as numeric results, will be presented in this section.

5.1. Evaluation of the operational conditions

Here, some conditions and limitations that we found during the experimental part will be explained:

5.1.1. Diffusion

Microfluidic is typically controlled by low Reynolds and high Péclet numbers and the mixing is determined by diffusion. [7] This diffusion is dominant if the Péclet numbers are smaller than 1000. A higher flow rate leads to higher Péclet numbers [29], what allows us to obtain a 50/50 flow.

In Table 1, the corresponding Reynolds and Péclet numbers for different flow rates, from both inlets combined, are calculated for the proposed active SAW mixer, with Sulforhodamine B diffusion coefficient of $4,7 \text{ m}^2/\text{s}$. [38]

For flows with Péclet numbers below 1000 (we include flows with $Pe \approx 1000$), the flow is diffusive dominant and on flows with Péclet numbers below 10000, diffusion can be perceived.

Flow rate (ul/h)	Flow velocity (mm/s)	Re	Pe
25	1,2375	0,089	263,3
50	2,475	0,178	526,6
100	4,95	0,356	1053,19
200	9,9	0,712	2106,38
400	19,8	1,425	4212,77
600	29,7	2,137	6319,15
800	39,6	2,849	8425,53

1000	49,5	3,561	10531,91
1200	59,4	4,272	12638,3
1500	74,25	5,341	15797,87
2000	99	7,123	21063,83
4000	198	14,25	42127,66
6000	297	21,367	63191,49

Table 1: Flow conditions, Reynolds and Péclet numbers

According to these parameters, flow rates over 94,9 $\mu\text{l/h}$ shouldn't be dominated by diffusion. Flow rates below this one present mixing due to diffusion. In Figure 24, we can observe a comparison between flow with Péclet numbers around 1000, and a flow rate over 10000, flow rates of 100 $\mu\text{L/h}$ and 1600 $\mu\text{L/h}$ (combining flows of both inlets, 50+50 $\mu\text{L/h}$ and 800+800 $\mu\text{L/h}$), where even though Péclet numbers are slightly over 1000, diffusion is still dominant.

In Table 1, the calculated parameters are referent to the total flow inside the microchannel, however, in the future of this report, when we mention a flow rate, we will refer to the flow rate correspondent to each inlet, this is, half of the total flow rate.

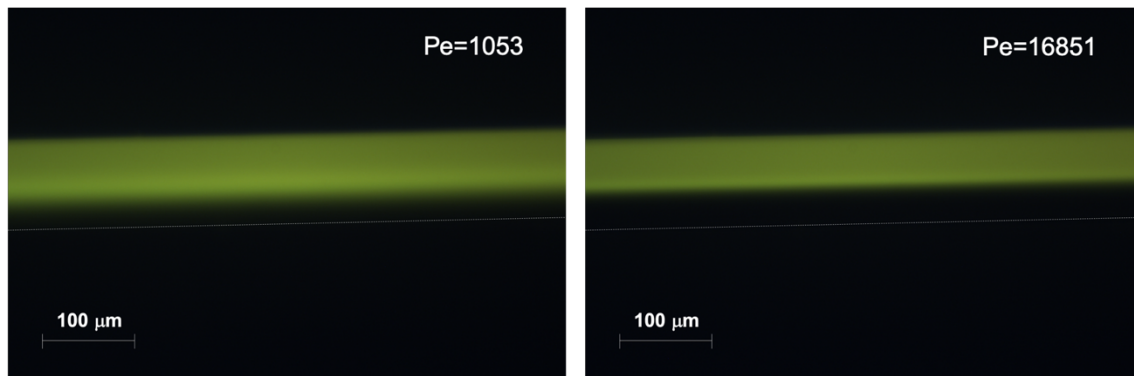


Figure 24: Diffusion comparison: Péclet numbers around 1000 vs. Péclet numbers over 10000

Using flow rates of 100 $\mu\text{L/h}$, we found that even though diffusion is not dominant, there is some mixing due to this and we don't get a 50/50 flow. The same happens until 400 $\mu\text{L/h}$, but it gets weaker as higher the flow rate is.

We also considered the possibility that diffusion may be affected by the concentration of solute. We tested how diffusion was affected in different scenarios, with different concentrations of solute. The experiment was done making solutions of

0,5%, 0,1% and 0,01% of Sulforhodamine B + DI water and using a flow rate of 100 $\mu\text{L/h}$ each stream.

In Figure 25 there is a comparison between the different solutions, being shown how the diffusion is affected by the concentration.

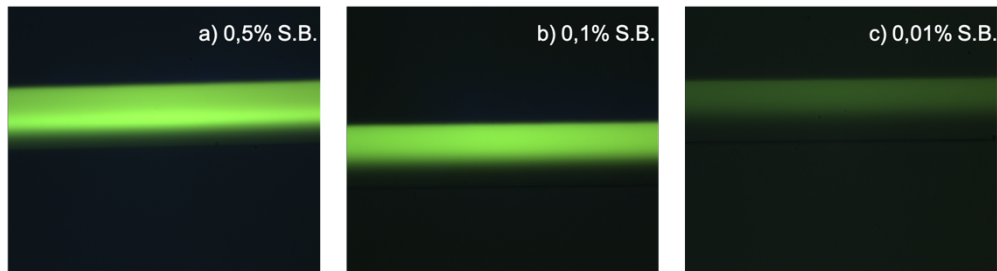


Figure 25: Comparison of diffusion with different concentrations

We can see how the diffusion effect gets weaker as the concentration decreases. We can also appreciate how the fluorescence gets less bright with the decreasing of the concentration.

Higher brightness in Figure 25 than in Figure 24 is explained due to this experiment was done with a microchannel bonded to a glass slice. Pictures in Figure 24 were taken during an experiment with the microfluidic mixer device, where microchannel is bonded to LiNbO_3 , this sample is attached to the SAW connector platform and, underneath, there is another piece of LiNbO_3 . The light through all these materials makes that the pictures look less bright.

Due to this effect, we chose 0,5% Sulforhodamine B concentration for experiments, even though the diffusion is higher than with other concentrations.

Considering all this, our experiments are done using flow rates in which diffusion is not dominant. This means that we will try to mix flow rates over 500 $\mu\text{L/h}$. We will try to reproduce, or getting as close as possible to the results obtained in recent publications. [29][30]

5.1.2. Occurrence of bubbles

The limitations in the power applied for mixing are conditioned by the appearance of air bubbles when a certain limit is exceeded. Running experiments, we have discovered that this handicap in the capability of power delivering is limited by the flow rate. It can't be set an specific limit for each flow rate, but it is always near the same value. As higher is the flow rate, as much power can be produced by the SAW generator without bubbles appearance. Using a Single IDT, with a flow rate over $5000\mu\text{L/h}$, the higher power that the SAW generator, with this design, is capable of produce, $2,57\text{W}$, can be applied without producing bubbles. Of course, $2,57\text{W}$ also is related to the mixing limit we can achieve with that flow rate.

It also was discovered that, in order to reduce this bubbles appearance and push this limit as far as we can, we have to do an slow power increasing. If the power is increased fast, bubbles will appear easily at lower powers.

In Figure 26 a picture of a bubble appearing in the microchannel after exceed the power limit during an experiment.

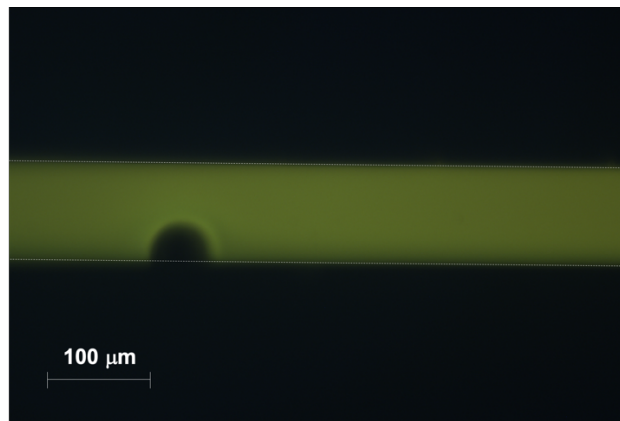


Figure 26: Bubble appearing inside the microchannel.

When bubbles start appearing 50/50 flow is ruined and one of the fluids full fill the microchannel, while the other one tries to recover its stream, until bubbles completely disappear. That is the scenario shown in Figure 16.

Considering this, a power limitation determined by bubbles appearing, we try to mix both fluids with the SAW produced by one IDT first, and then by two. The

different experiments are done changing the flow rates (flow rates are always the same for both fluids)

5.1.3. Dual IDT high power limitation

Another limitation we had to face running the experiments was applying high power to both IDTs. When we did so, we discovered that the substrate could not handle it and it broke. Two samples were ruined when we got close to 1,5W per IDT, so we decided to not push further than 1W per IDT in future experiments. This is a problem that should be study in future stages of the project.

In Figure 27 is shown a picture of a broken sample after we overpassed the power limit:

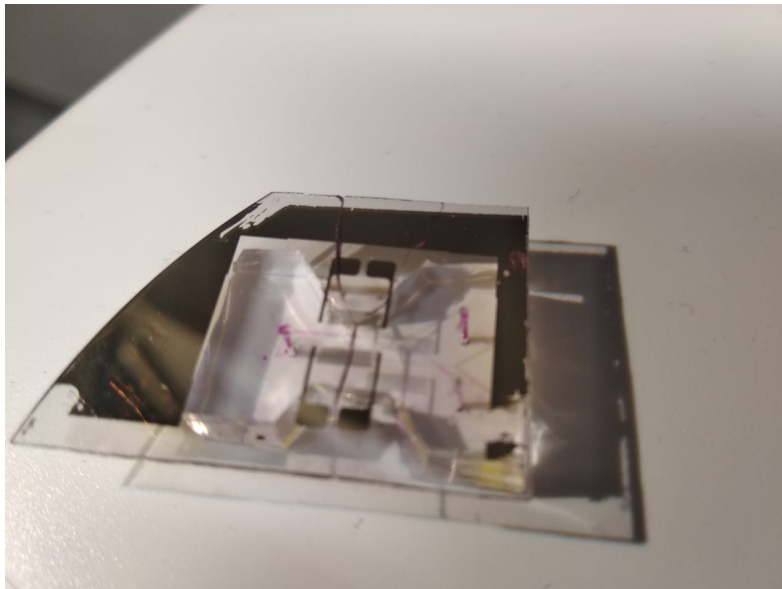


Figure 27: Broken sample after overpassing power limit

The crash all along the substrate can be appreciated through the center of the mixer.

5.2. 80 MHz mixer:

In this part, mixing produced by the 80MHz mixer will be studied, for flows where diffusion is not present. It is desired to do a comparison of our device with recent publications where they achieved a high level of mixing from 600 μ L/h (using a Dual IDT)[29] to 6000 μ L/h (using a chamber and a focused IDT) [30]. Our mixers are made with two IDTs, in order to be able to use both for mixing and, at some point in further work, producing Standing Surface Acoustic Waves for nanoparticles separation [39]. However, firstly, our intention is to test the mixing capacity of a Single IDT and then compare it with the Dual IDT capacity. Power will be limited by bubbles appearance, in the case of Single IDT mixing and by breaking limit in Dual IDT mixing scenario.

5.2.1. Single IDT performance:

Experiments were done using Violet and Green light and testing different samples. The results presented here were obtained using the one shown in Figure 28.

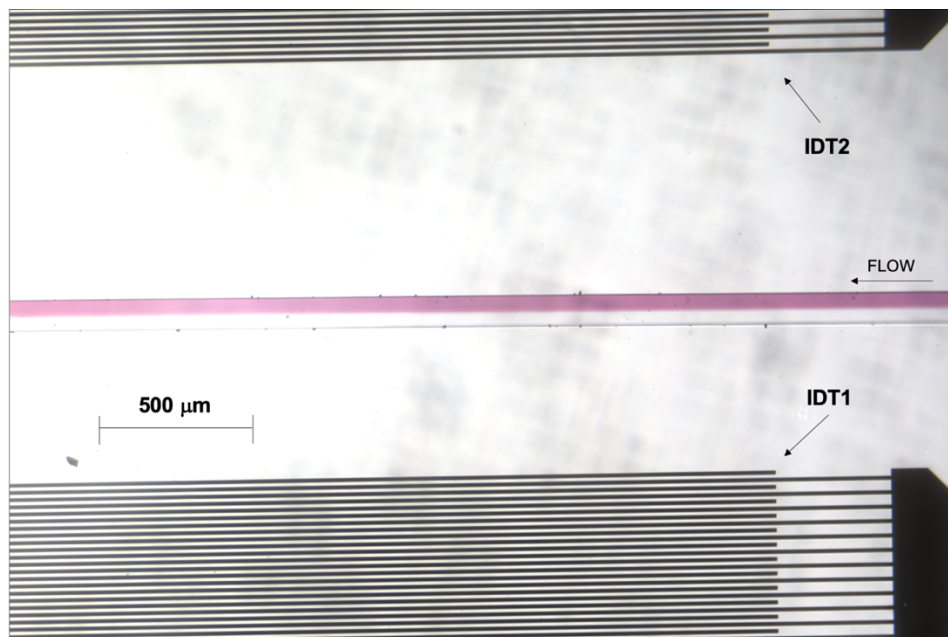


Figure 28: Microchannel and both IDTs. Microscope + regular light

As the distance from IDT1 to the microchannel is smaller than from IDT2 to this one, we will start testing it and after, we will do the same for IDT2. Then we will compare their performances so we can determine how important is the distance for mixing.

5.2.1.a) IDT1 performance

Here there will be shown the results obtained using IDT1. Mixing of a flow rate of $400\mu\text{L/h}$ is also studied as it is in the limit where diffusion is noticed.

- **$400\mu\text{L/h}$:**

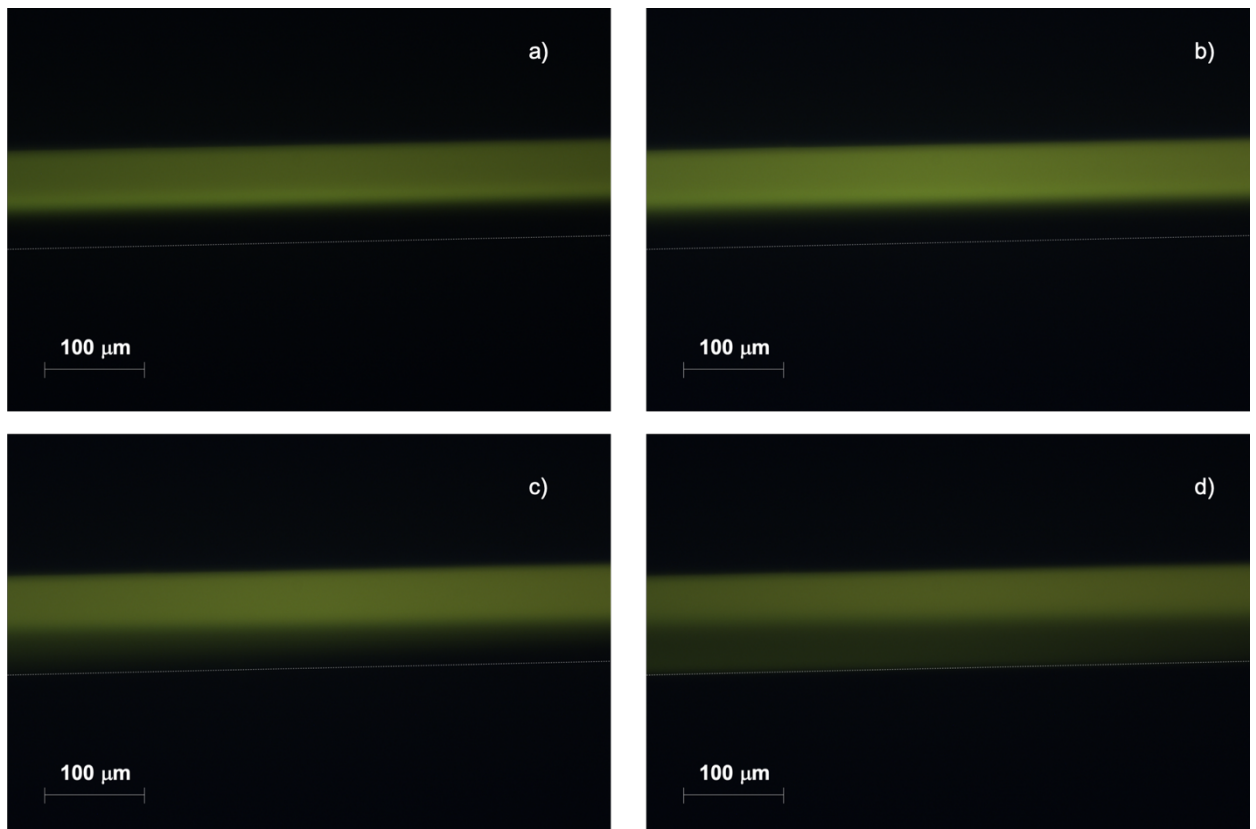


Figure 29: Mixing of $400\mu\text{L/h}$ using violet light: a) 0W; b) 500mW; c) 1W; d) 1,5W

In Figure 29, it is seen the mixing of 400 μ L/h with a) 0W; b) 500mW; c) 1W; d) 1,5W . In Figure 29.a) there is no mixing, even though, some diffusion can be detected. 1,5W represent the limit of power that we can deliver with flow rate of 400 μ L/h, if we increase this, we rapidly start producing bubbles.

- **600 μ L/h:**

In Figure 30 we can see how mixing increases as power does. There is a power limitation in 2W, after that bubbles start appearing. Even with 2W, if you keep delivering that power for a long time bubbles might start showing up.

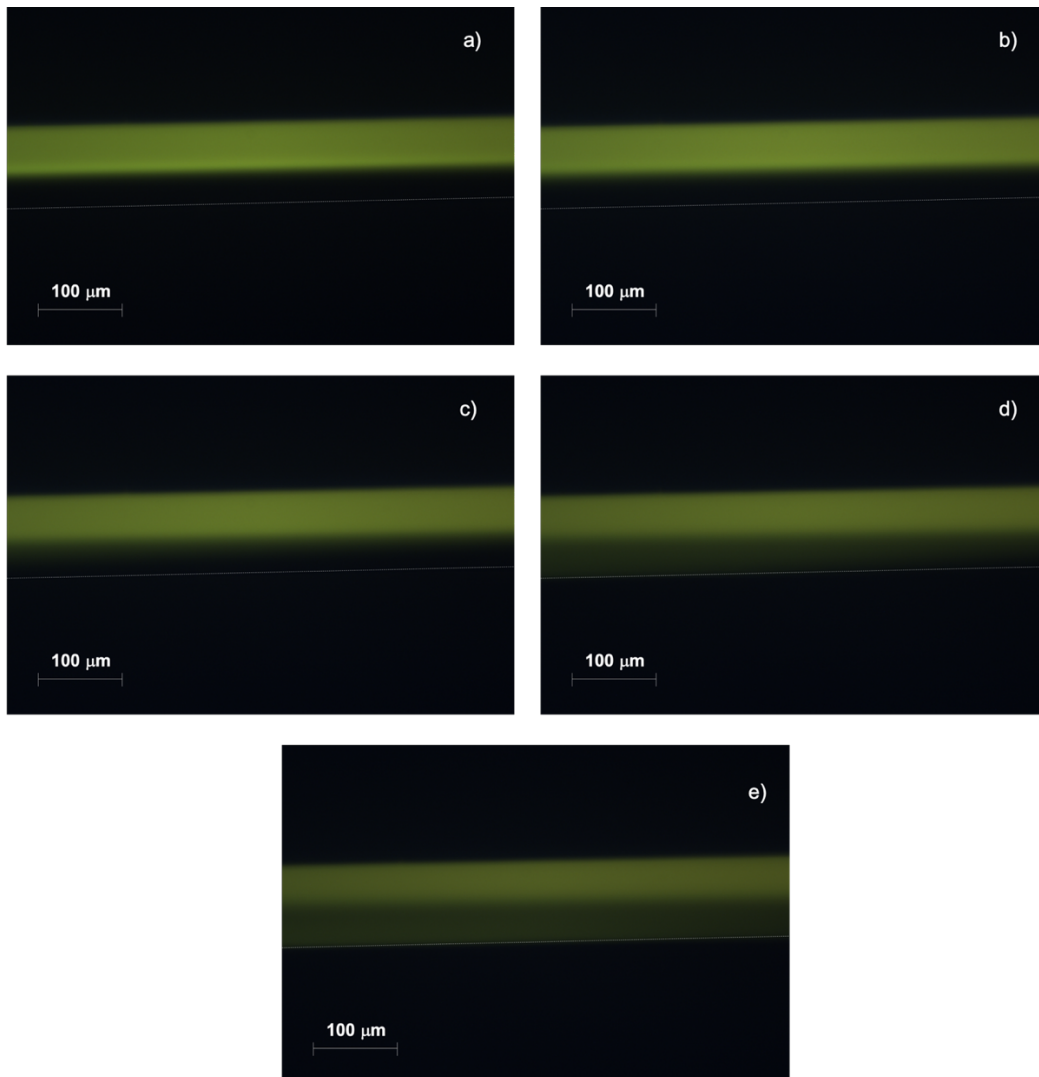


Figure 30: Mixing of 600 μ L/h using violet light: a) 0W; b) 500mW; c) 1W; d) 1,5W; e) 2W

- **800 μ L/h:**

With this flow rate, there is no mixing with 500mW of power, therefore it is not included in the images of Figure 31.

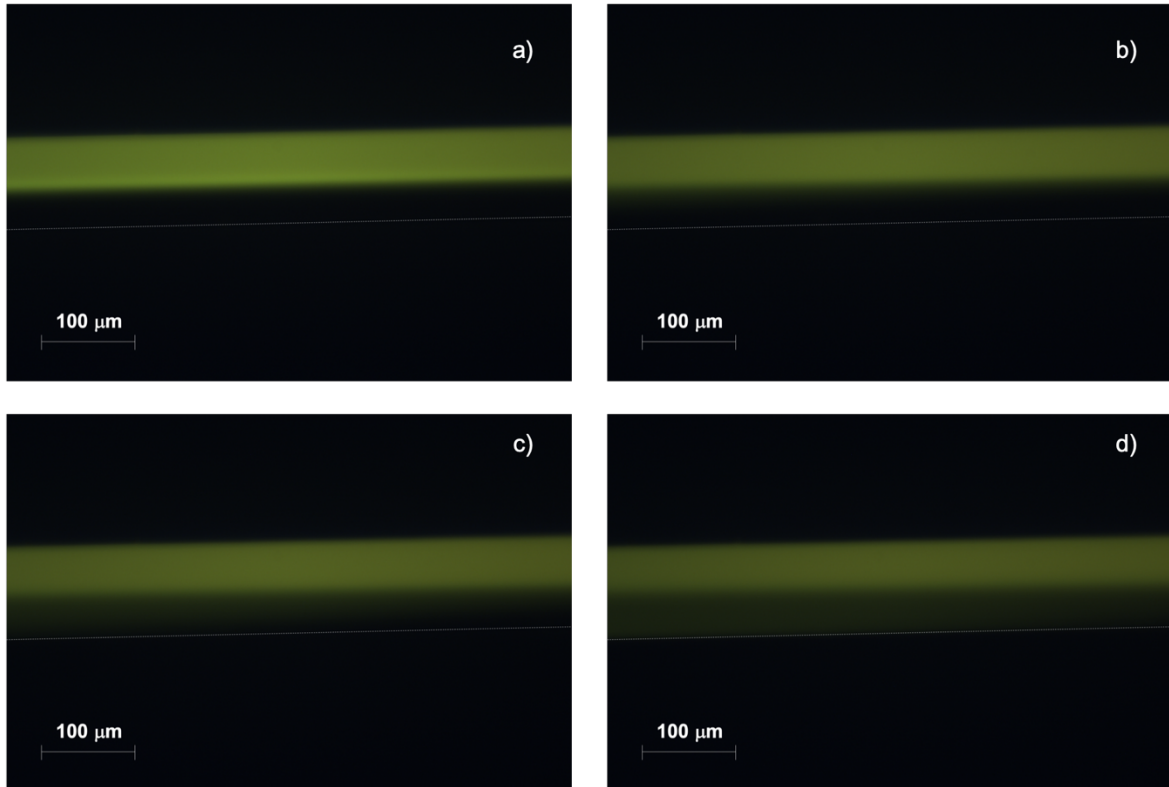


Figure 31: Mixing of 800 μ L/h using violet light: a) 0W; b) 1W; c) 1,5W; d) 2W

In Figure 31 pictures of mixing with 1 , 1,5 and 2 W is shown, for a flow rate of 800 μ L/h.

- **1000 μ L/h:**

Experiment, using violet light, for mixing of a flow rate of 1000 μ L/h, is shown in Figure 32

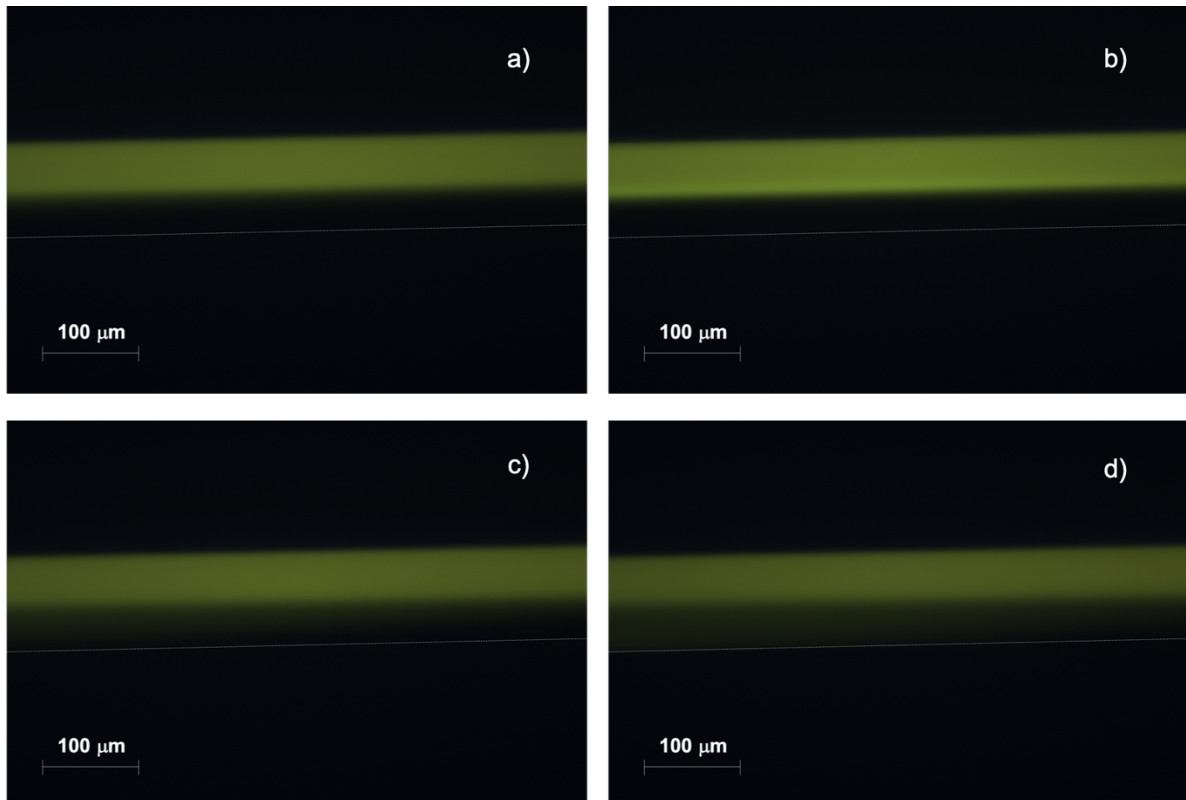


Figure 32: Mixing of 1000 μ L/h using violet light: a) 0W; b) 1W; c) 1,5W; d) 2W

In Figures 29, 30, 31 and 32, it is possible to appreciate how the lower power applied, induces some stirring in the fluid and when we overpass the **hhh**, we start producing some actual mixing

After this, we tried the experiment at really high flow rates and maximum power, in order to see how much mix we could achieve. For this we used flow rates of 1500, 2000 and 6000 μ L/h.

- **High flow rates: 1500 μ L/h, 2000 μ L/h, 6000 μ L/h**

In Figure 33 is shown the mixing achieved using 2,57W, the maximum power for this design, for high flow rates.

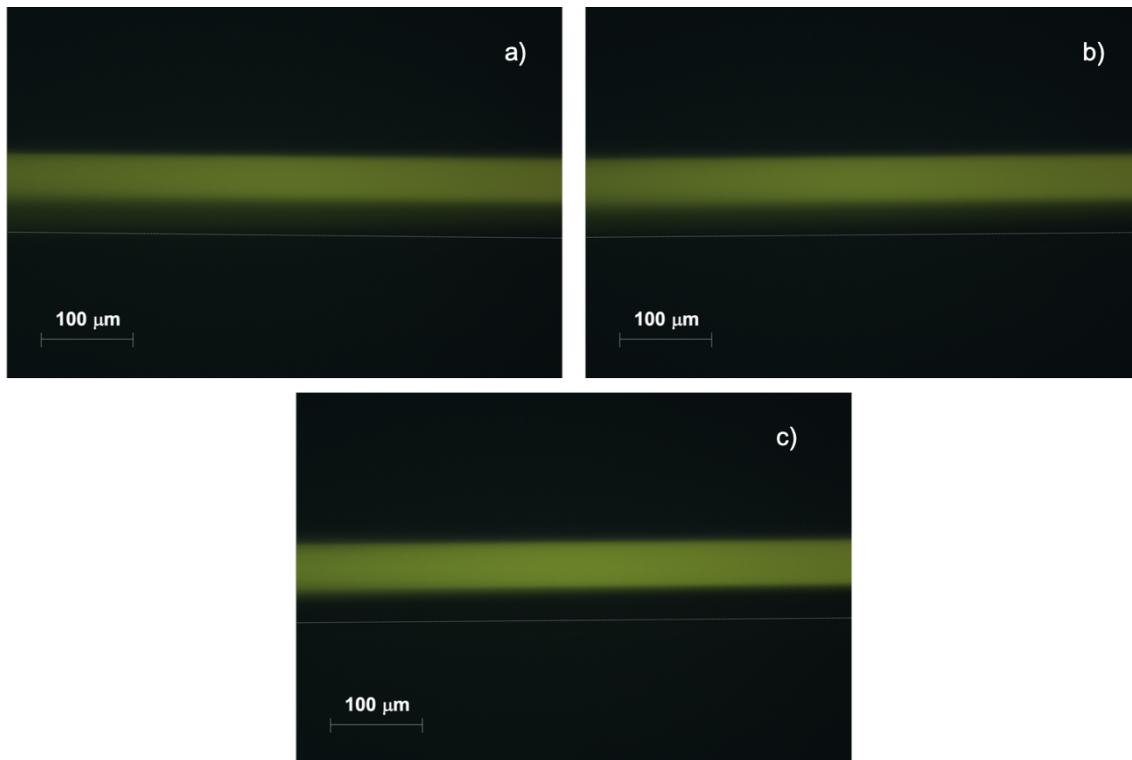


Figure 33: Mixing at maximum power, 2,57W for high flow rates, using violet light: a) 1500 μ L/h; b)2000 μ L/h; c)6000 μ L/h

Once this experiment was done, we decided to repeat it using another light wavelength, in order to improve the contrast of colours in the pictures and, perhaps, get better results after image processing.

For this, we adjusted the intensity and the acquisition of the light source. We used Green light for fluorescent excitation, obtaining a higher contrast of results. Of course, the intensities of the light and the acquisition times are different, being both parameters higher for the Violet light. In Table 2, parameters using for imaging are specified.

Light	Wavelength (nm)	Intensity (%)	Acquisition time (us)
Violet	470	100	150000
Green	550	70	25000

Table 2: Light source parameters comparison

At the first time, Green light wasn't used because the brightness was too high, so, for this, we did a parameter adjustment.

In Figure 34, there is a comparison of images taken using Violet and Green light, for the same flow rate and power, with the same device:

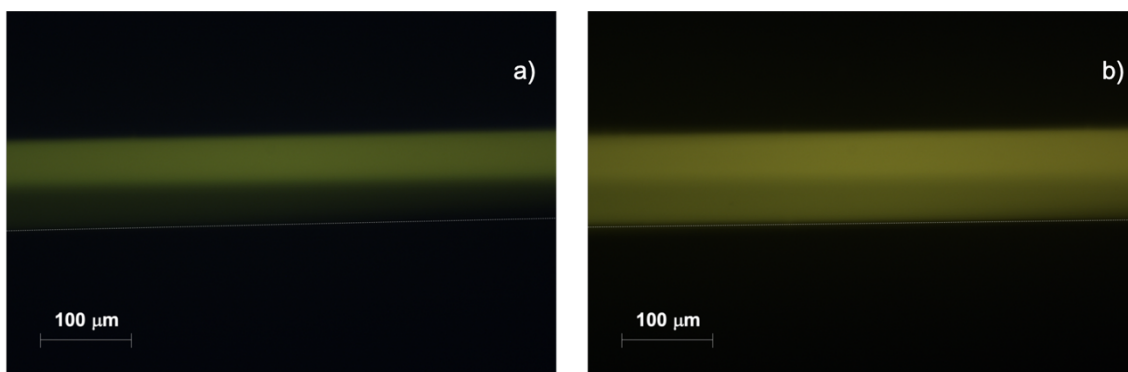


Figure 34: Image comparison for 1000μL/h and 2W: a) Violet light; b) Green light

As we can see in Figure 34, the colour intensity is much higher in image b), then we can expect a better result when the images are processed.

Same procedure, as the previous, was done using same flow rates and powers for mixing. In order to not doing the same picture presentation as before with the new images, we will show a comparison of them for the two different light wavelengths, as we did in Figure 34.

▪ 600 μ L/h:

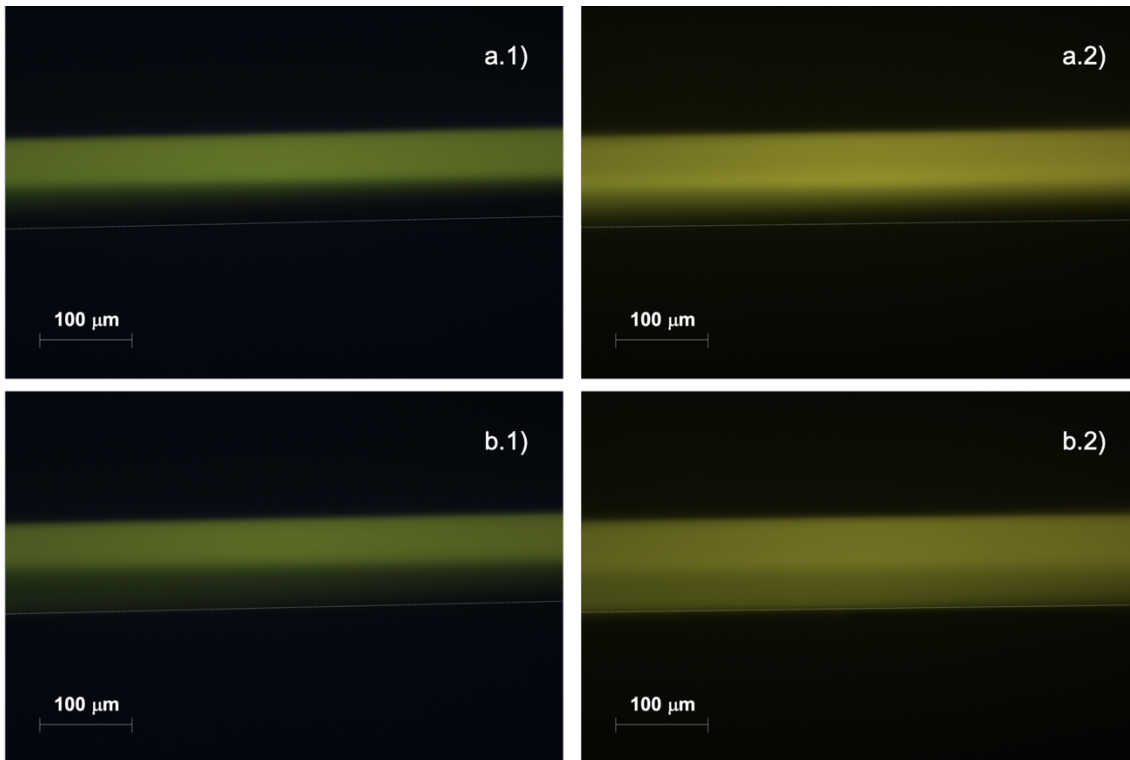


Figure 35: Mixing comparison of 600 μ L/h. Violet light vs. Green light: a) 1W; b) 1,5W

In Figure 35, there is a comparison of mixing of 600 μ L/h. Images a.1) and a.2) show the mixing of this flow rate with 1W of power, under Violet light in the number 1 and Green light in the second one. Images b.1) and b.2) show the mixing of 600 μ L/h with 1,5W of power, under Violet light in the number 1 and Green light in the second one.

▪ 800 μ L/h:

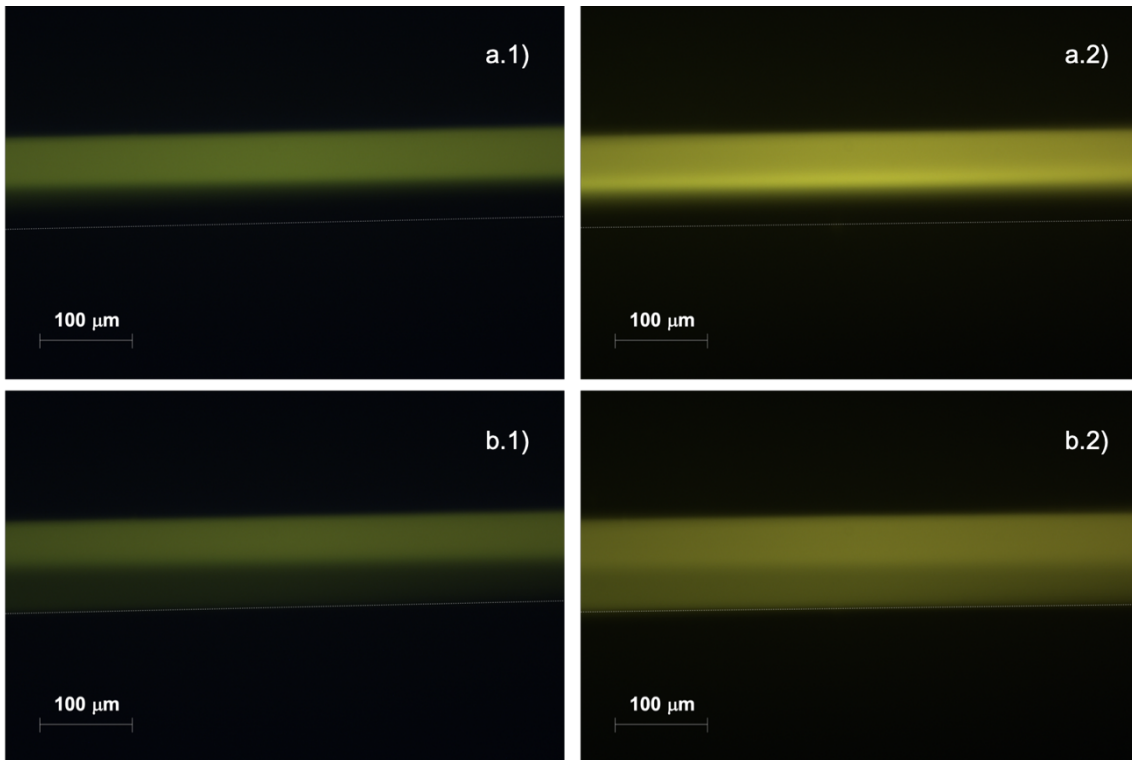


Figure 36: Mixing comparison of 800 μ L/h. Violet light vs. Green light: a) 1W; b) 2W

In Figure 36 is shown the mixing comparison of 800 μ L/h with 1W in images a.1) and a.2) and 2W in images b.1) and b.2). Violet light is used in pictures a.1) and b.1) and Green light in pictures a.2) and b.2).

▪ **1000 μ L/h:**

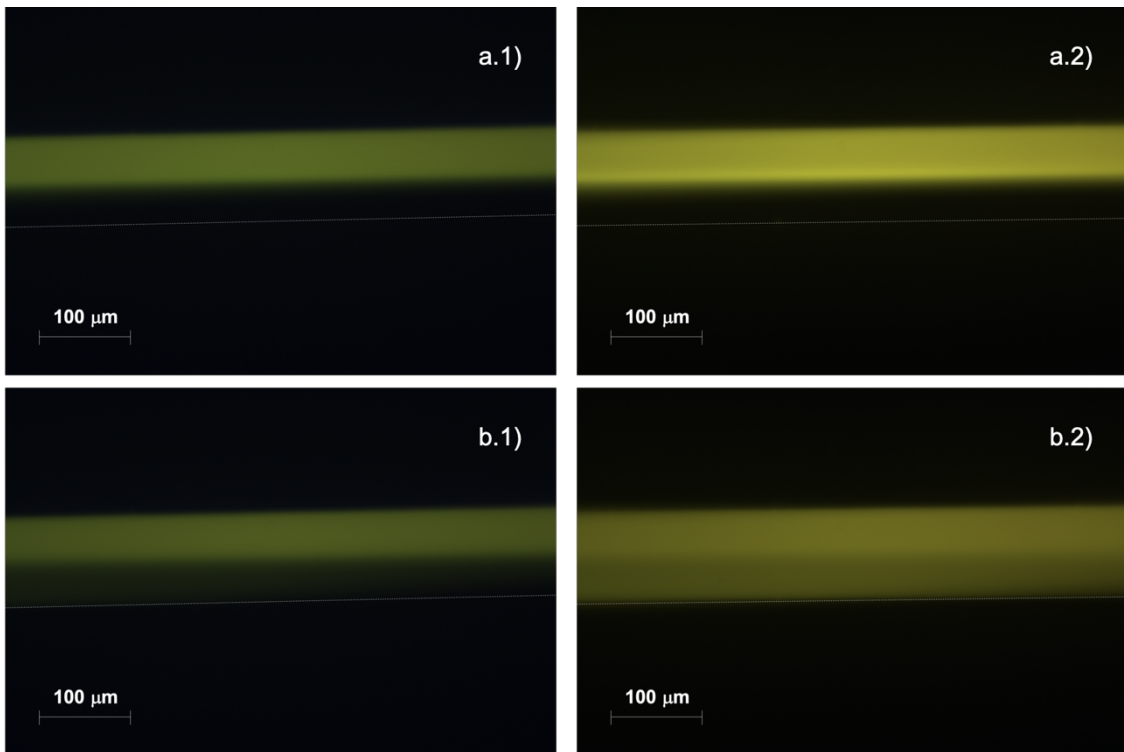


Figure 37: Mixing comparison of 1000 μ L/h. Violet light vs. Green light: a) 1W; b) 2W

In Figure 37 is shown the mixing comparison of 1000 μ L/h with 1W in images a.1) and a.2) and 2W in images b.1) and b.2). Violet light is used in pictures a.1) and b.1) and Green light in pictures a.2) and b.2).

- **High flow rates: 2000 μ L/h and 6000 μ L/h**

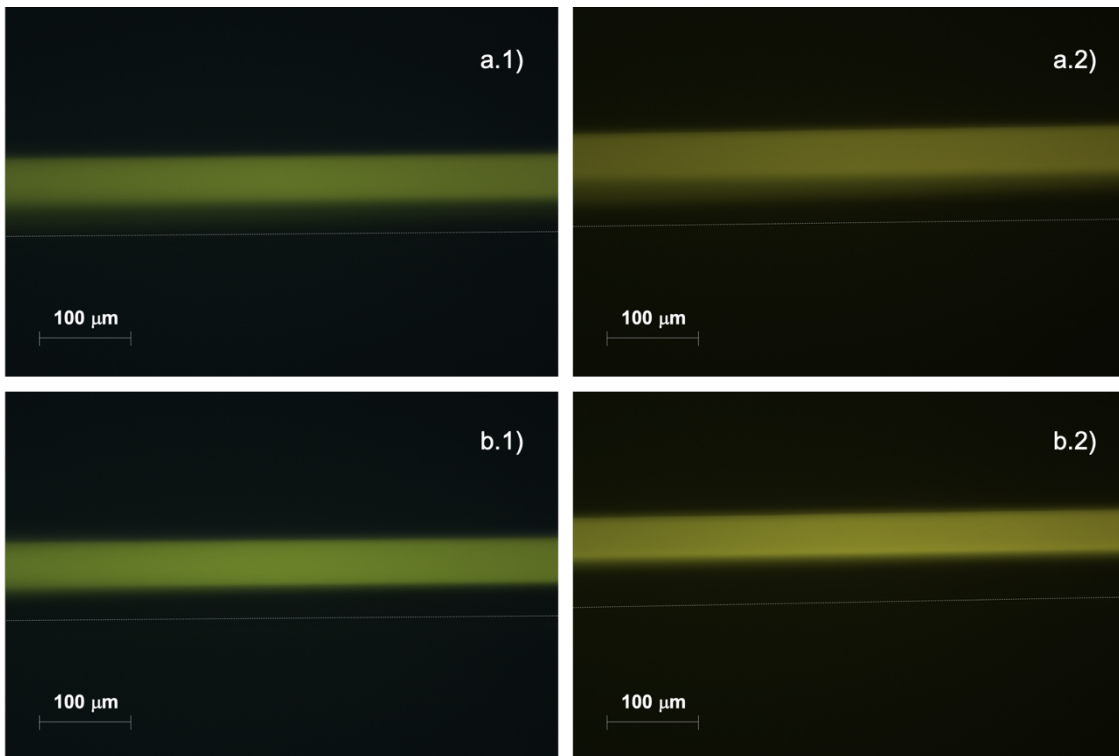


Figure 38: Mixing comparison of high flow rates at maximum power, 2,57W. Violet light vs. Green light

Figure 38 shows a mixing comparison under Violet light [a.1) and b.1)] and Green light [a.2) and b.2)]. Images a.1) and a.2) show the mixing of 2000 μ L/h using 2,57W. Images b.1) and b.2) show the mixing of 6000 μ L/h using 2,57W.

Mixing capability at high flow rates is low as we observe in Figure 38, however, we wanted to test it in order to do a comparison with other publications where these flow rates are mixed.

As a summary of this part, we determined that mixing can be better appreciated when using Green light. We could achieve mixing from 600 to 1000 μ L/h when high power is applied, limited by the bubbles appearance. When applied power is below certain limit, we can see some fluid stirring and over that limit, laminar flow is broken and mixing starts occurring. Mixing at flow rates from 1000 to 2000 μ L/h will be study in the future of the project.

5.2.1.b) IDT2 performance:

The next experiment was done using IDT2, in order to do a mixing comparison rely to the distance from the IDT to the microchannel. As we said before, IDT1 was almost half the distance to the microchannel than IDT2. With this experiment we will test how this difference affects to the mixing.

Using the same parameters as for IDT1, we try to mix the two fluids producing SAW trough IDT2. According to a recent paper by Zhang et al. from 2019 [40], based on previous studies [41], the energy transfer through the substrate and fluid, leads to a SAW attenuation, related to the length and substrate and fluid density. It also exists a wave attenuation related with PDMS [31], but it should affect them equally. We will do a comparison of images and, when images are processed, a results comparison, so we can see how much mixing is affected by the distance to the fluid.

With a flow rate of 600 μ L/h:

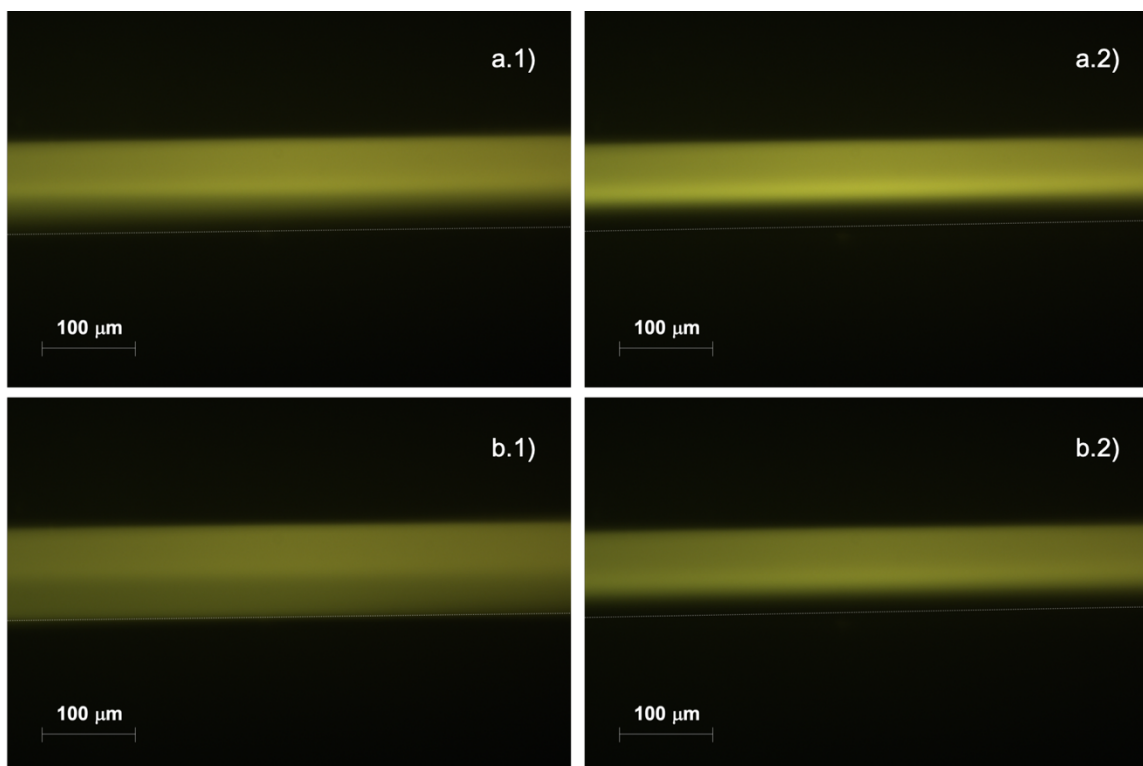


Figure 39: Comparison performance IDT1 vs. IDT2

In Figure 39, we show a comparison of mixing performance between IDT1 and IDT2, for the same flow rate, 600 μ L/h. Images a.1) and a.2) show the mixing produced by 1W of power, corresponding to IDT1 and IDT2 respectively. Images b.1) and b.2) correspond to mixing produced by 1,5W by IDT1 and IDT2 respectively.

As we can clearly see in Figure 39, mixing produced by IDT2's performance is quite lower than the one produced by IDT1.

5.2.2. Dual IDT performance:

Basing us on an article from 2013, made by Myeong Chan Jo and Rasim Guldiken [29], we want to determine how much we can improve mixing using a Dual IDT, compare to a Single IDT. For this, as it has been done for the whole project, an image comparison will be done and, next, Matlab will be used to obtain a more precise comparison.

In this experiment, it will be compared the mixing produce by IDT1, of the sample used before, with the mixing produce by IDT1, using the same power than before, plus the mixing produced by IDT2. Unfortunately, this experiment was done before starting using the new light wavelength, Green color, and the sample was ruined before we could repeat it. We had no time to fabricate a new one, so we only have images with the Violet light, anyway, comparison can be done with them.

Performing this experiment, we also found that producing bubbles is easier than using only one IDT, so the power increasing must be more careful and, when it is possible, should be done with both IDT's at the same time. This is because if an IDT is kept producing SAW, with a relative high power, as 1W, while the other's IDT is increased, the chances of producing bubbles are bigger than when both are slowly increased at the same time.

A power limitation was also found in this experiment. High power can't be produced by two IDTs, in a way that if this is done, most likely the substrate will crash.

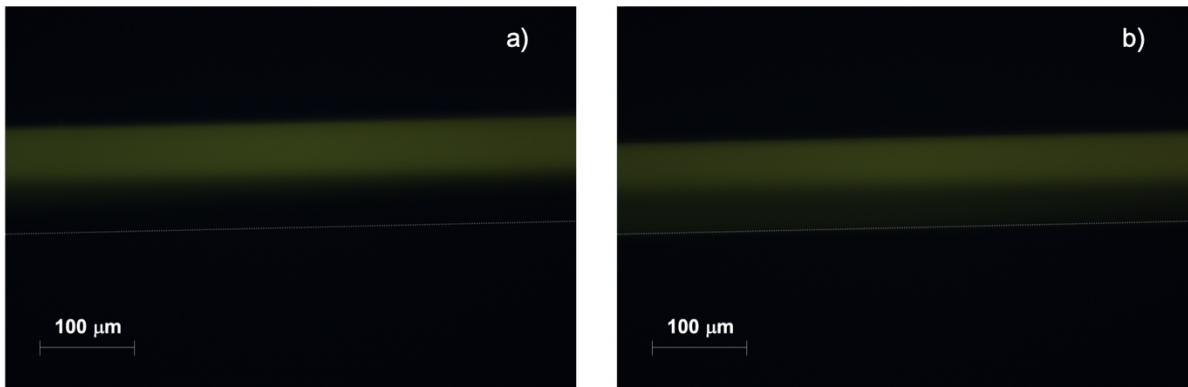


Figure 40: Single IDT vs Dual IDT mixing of 600 μ L/h comparison.: a) 1W and 0W; b) 1W and 500mW

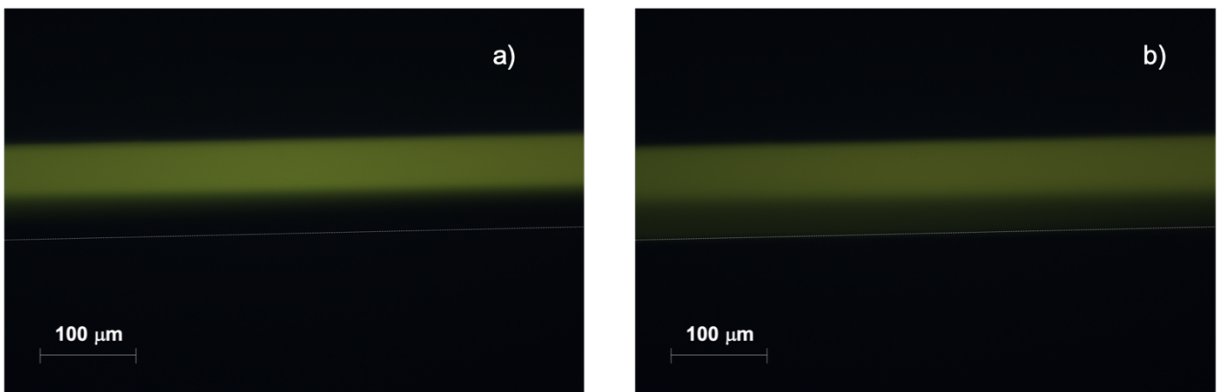


Figure 41: Single IDT vs Dual IDT mixing of 800 μ L/h comparison.: a) 1W and 0W; b) 1W and 700mW

In Figure 40, it is shown the mixing difference using one or two IDTs for 600 μ L/h, using a single IDT with 1W in a) and using two IDTs with 1W and 500mW in b). In Figure 41, it is shown the mixing using 1W and 1W/700mW, respectively for a) and b).

In both pictures, it looks clear how the mixing is increased when both IDTs are working together, compare to when only one IDT is used. In the next part of the report this difference in mixing capacity will be studied deeper.

Running this experiment two samples were damage with no possibility of fabricate any more. This is because the substrate can't handle a high power from both IDTs, so when we did this, the substrate broke in half.

5.3. Other designs mixers

As we said, we made other two IDT designs to be fabricated. We got fabricate samples with both designs, of 120 and 40MHz.

5.3.1. 120MHz mixer

The testing of this device wasn't as we expected. As it was explained, its fabrication was quite more delicate than with the other designs, due to the tiny size of the features of the IDTs. This issue made even more difficult to get a functional Dual IDT than with the 80MHz one, so it could not be achieved. Therefore, this experiment could only be done using a Single IDT.

The procedure for the experiment was the same as for the previous ones:

- **600 μ L/h:**

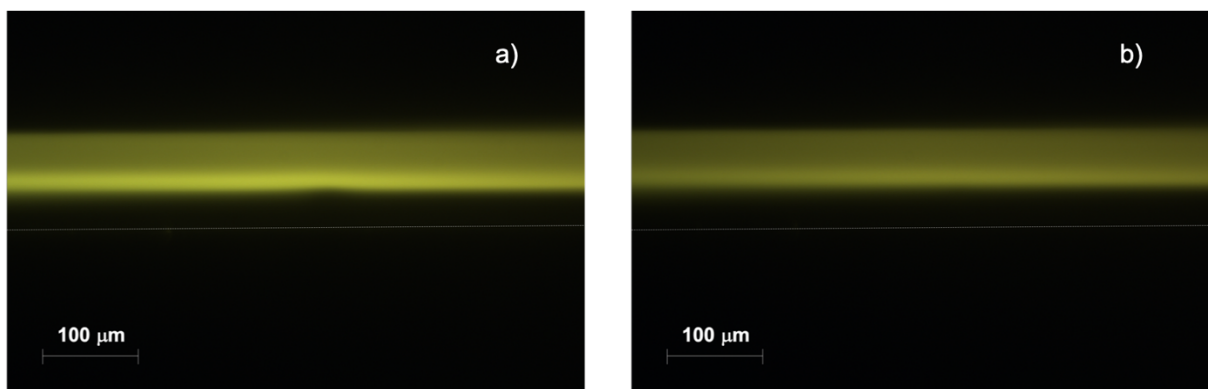


Figure 42: Mixing comparison of 600 μ L/h using a 120MHz mixer: a)0W; b)2W

Figure 42 shows the mixing of 600 μ L/h produced by 2W using a 120MHz mixer, compared to no mixing.

- **800 μ L/h:**

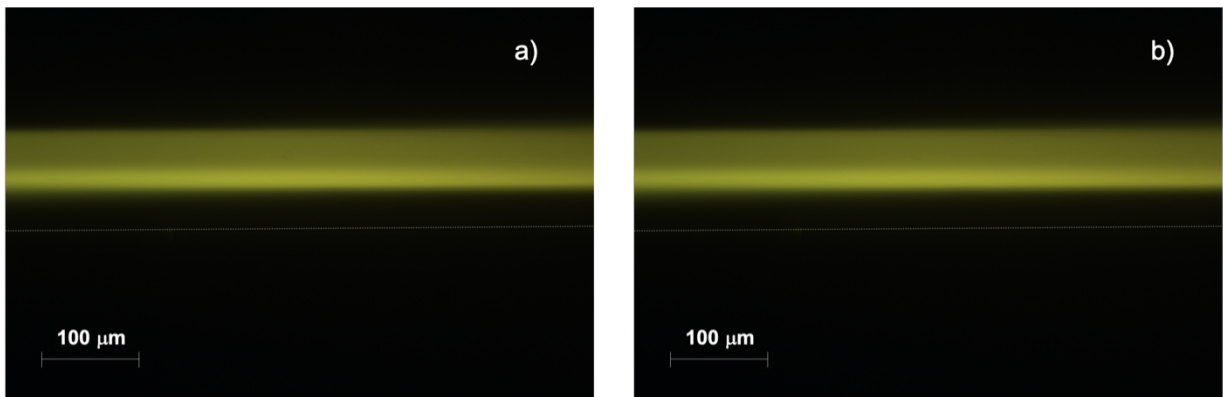


Figure 43: Mixing comparison of 800 μ L/h using a 120MHz mixer: a)0W; b)2W

In Figure 43 we can see the mixing of 800 μ L/h produced by 2W using a 120MHz mixer, compared to no mixing.

In both scenarios, it can be barely appreciated that anything is occurring, or even nothing does. The experiment was repeated with different flow rates and power and mixing wasn't achieved. It was noticed that when the IDT was activated, some pulse occurred but not proper mixing as for the 80MHz device. This design will be study more deeply in a further stage of the project.

5.3.2. 40MHz mixer

The 40MHz mixer was fabricated but for external causes it could not be tested. This task will be performed in a next stage of the project and its results will be compared with the obtained in this work.

5.4. Analysis of mixing

Image processing for analysing the mixing was performed using Matlab, with two different scripts, one for each kind of pictures taken, with Violet and Green light. Experiments were done on different days, so the position of the images is not equal, but the procedure is the same.

The scripts use an image of the microchannel, full of water, as water is colourless, as a microchannel size reference, being the image divided in 800 pixels. Figure 44 is the one we used.

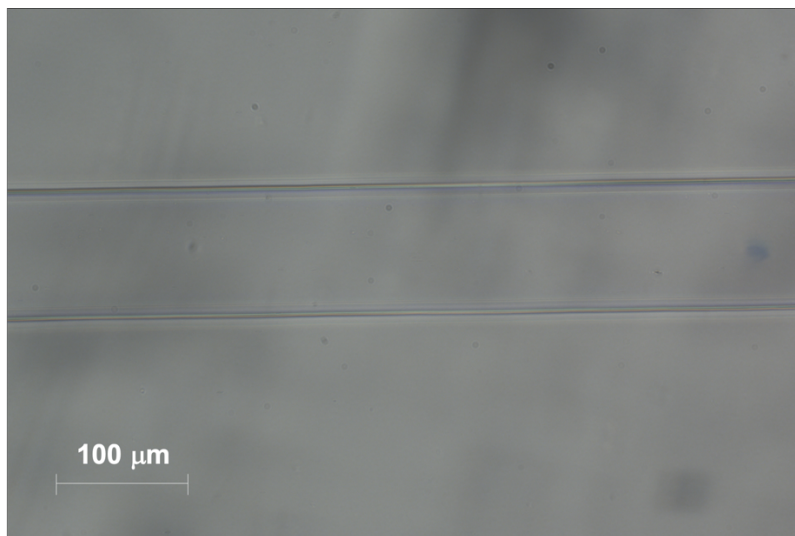


Figure 44: Microchannel full with water. Regular light

Once we have the size reference, the script turns all the pictures into grey, so the intensity of each pixel is measured in a grey scale. The image with no power applied, no mixing, is used as a minimum reference. Figure 45 is the image with no mixing turned into grey that will be used as a reference.

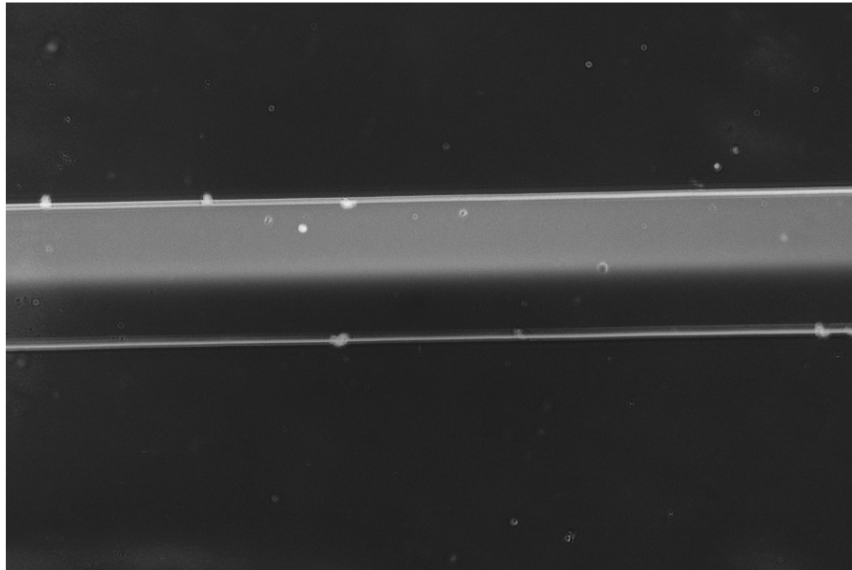


Figure 45: No mixing image used as a reference in Matlab

In Figure 46 are all the images with different power are turned into grey, to measure its intensity and plot the results.

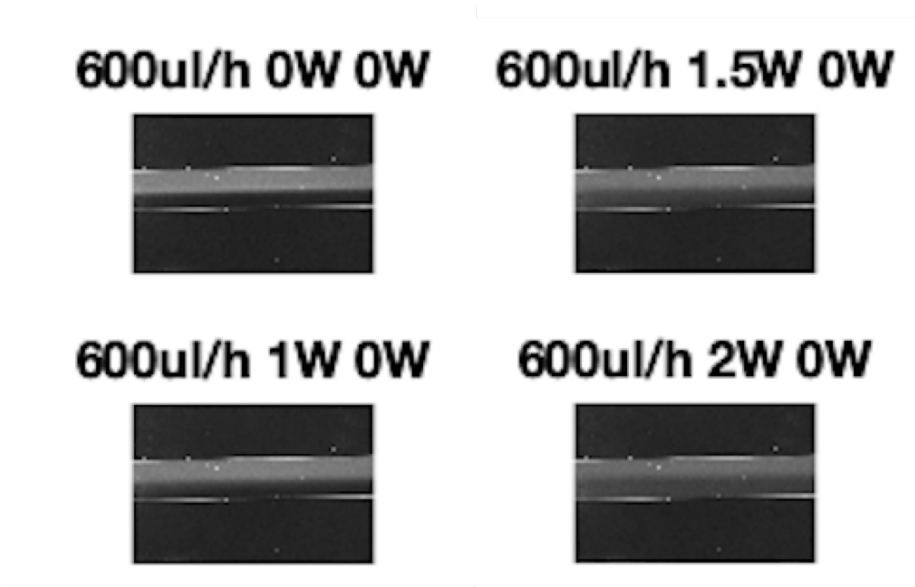


Figure 46: Different mixing images in grey, made by Matlab

Then, Matlab does an intensity measure of the pixels for each image, only in the space between the microchannel's limit, and makes a plot intensity vs. channel width (in pixels) of those measurements, getting as results Figure 47 and Figure 48:

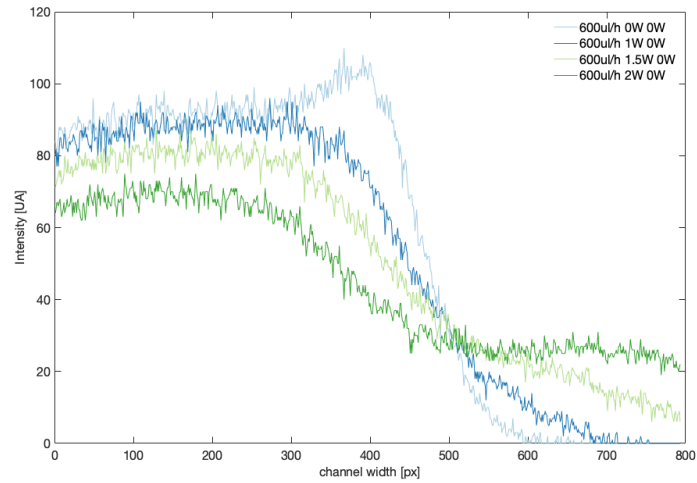


Figure 47: 600 μ L/h mixing curves using Violet light

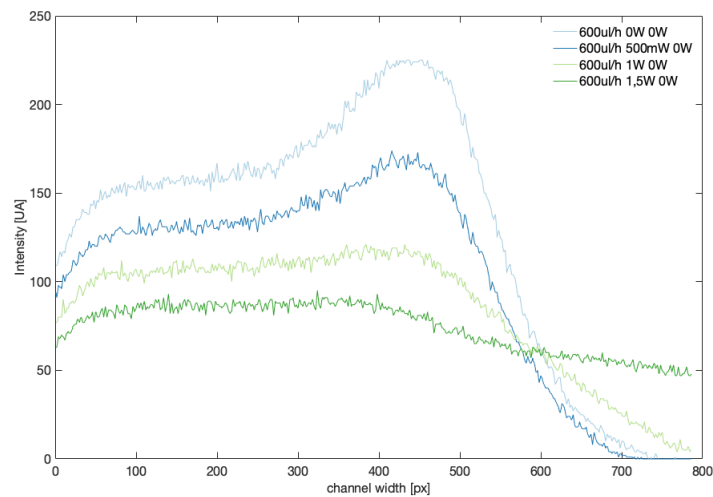


Figure 48: 600 μ L/h mixing curves using Green light

As we can observe, the shift from one curve to another, in the plot made using images taken with green light, is bigger, due to the higher intensity. However, the curves are not as sharp as the ones in the plot made using Violet light. Both results will be presented in this part of the report, but for the calculations of the percentage mixed we will use the second one.

It will be done so. As we shown in the comparison figures in the part of Experiments, in the first images some mixing wasn't visible due to the low intensity of the fluorescent emission. Therefore, the Green light one would show a more representative result.

In Figure 47 and Figure 48, we can see how the no mixing curve starts rising as it approaches the two fluid joint point, as we observe, in both kind of images, a brighter line at that point. We also observe a difference in the point where the curve drops, in a way that for Violet light images it occurs at the middle point, while in the Green light ones, as the brightness is higher, it occurs further.

A shift to the left is observed in Figure 48 between the 0W and the 500mW curve. This phenomenon occurs due to, at this point, power is not high enough for breaking the laminar flow and mixing the fluid. Instead of this, the effect of the SAW, too weak for mixing, is pushing the water towards the other side of the microchannel as the waves come from the water side, produced by IDT1.

Observing the plots, we see how the curves get more and more horizontal as the power increases, and so the mixing does. Considering this, we could say that 100% mixing is achieved when the curve is completely horizontal, this is, when the intensity is homogeneous in the whole microchannel. This value should be the same for all every plot, because 100% mixing should look the same independently of the flow rate, therefore, one single 100% mixing value will be obtained from all the means done. For 600 and 800 μ L/h, the mean was 72 approximately, for 800 was around 68, because of this, we decided to set this value on 70, for representing the 100%. For mixing quantifying, a mean of the most horizontal curve would represent, approximately, the 100% mixing value as this curve tends to this from both sides of it. While, the mean of the same curve, from the middle point to the end, where there was no fluorescent when power wasn't activated, would represent the quantity of mixed fluid, therefore, we could do a percentage of mixing using both values. Note that this percentage is just an approximation, not an accurate value.

The second experiment, using Green light, was done for flow rates where diffusion wasn't noticed, therefore we don't have data for 400 μ L/h and, so, mixing won't be quantifying, anyway the mixing process, using Violet light, will be shown for this flow rate. We will study our results from the flow rate where diffusion is no detectable, 600 μ L/h. This flow rate is the one which [29] achieved to 100% mix and we want to reproduce. Firstly, Single IDT performance will be study, then, the comparison of IDT1 vs. IDT2 will be shown and, finally, a comparison between Single IDT and Dual IDT.

5.4.1. Single IDT

Here, mixing produced by a Single IDT will be study and quantified. 400 μ L/h experiment is presented but not quantified, as some diffusion is acting on it.

- **400 μ L/h:**

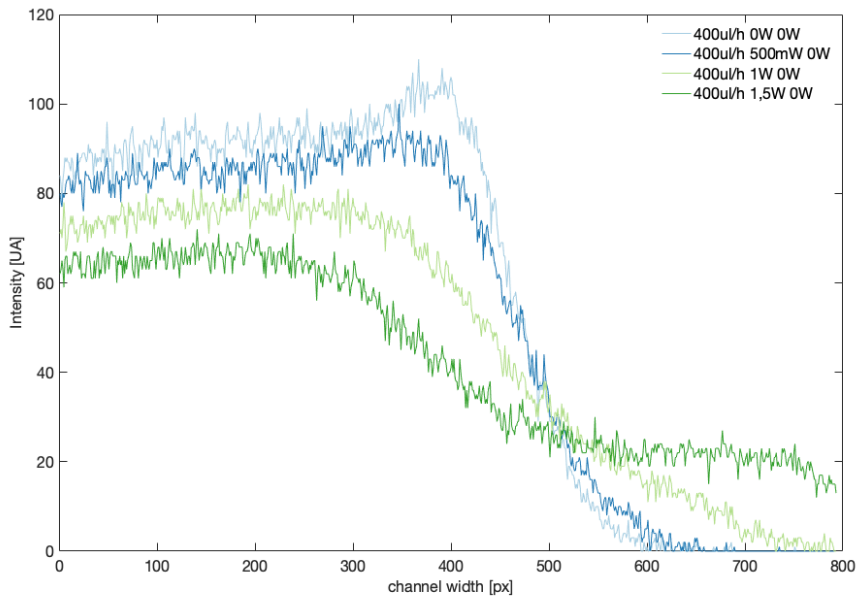


Figure 49: 400 μ L/h mixing curves, using Violet light

Figure 49 shows the mixing produced by one IDT for a flow rate of 400 μ L/h, where diffusion still produces some mixing, therefore, it won't be studied.

- **600 μ L/h**

Figures 40 and 41, shown before, represent the mixing produced by a Single IDT on a flow rate of 400 μ L/h. 2W power mixing is lacking in the Green light experiment because, this time doing it, bubbles appeared when we were close to this value, so getting a representative image was not possible. Anyway a really high mixing was achieved using 1,5W.

As we said, 70 will be used as the approximate reference value for 100%, based on the different means obtained. Mixing value for the 1,5W curve was 63,41. With 70 set as 100% mixing, the mixing produced by 1,5W could be estimated, on 600 μ L/h, around a 90%. Using 2W of power, we could say that we would be really close of achieving a 100% mixing. This flow rate, was the higher where Myeong Chan Jo et al. [29] could achieve 100% mixing, using a Dual IDT mixer. We are close of achieving it using a Single IDT.

▪ **800 μ L/h:**

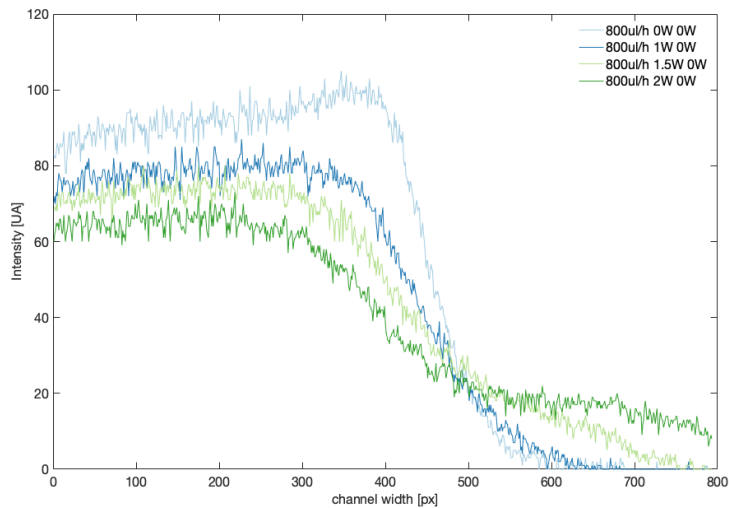


Figure 50: 800 μ L/h mixing curves, using Violet light

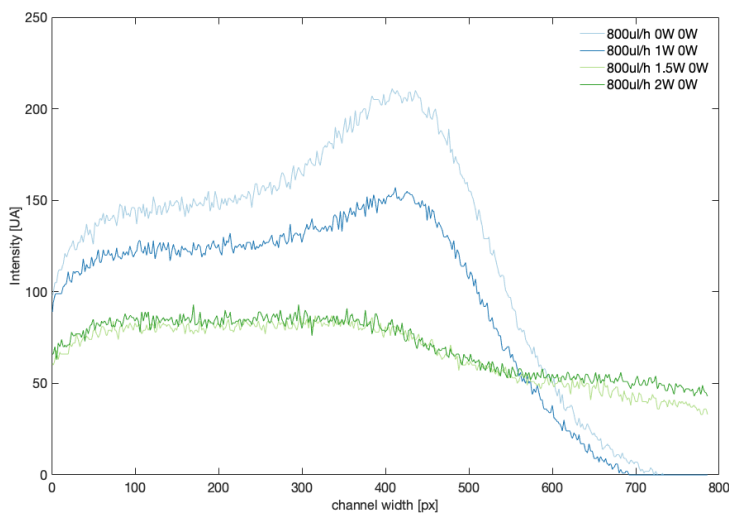


Figure 51: 800 μ L/h mixing curves, using Green light

Mixing curves of 800 μ L/h are shown in Figure 50 and 51. 1,5W and 2W curves are really close each other on the Green light plot. We can see that the difference between them is not as big as in the other plot, perhaps due to flow conditions at the moment when the pictures were taken. We can also see how 1W produces just a shift in the intensity, it is not enough for producing mixing.

Using 70 as 100% mixing reference, with a curve mean, from 400 to 800 (px), of 59, we estimate a mixing of around 85% for 800 μ L/h with 2W of power.

- **1000 μ L/h:**

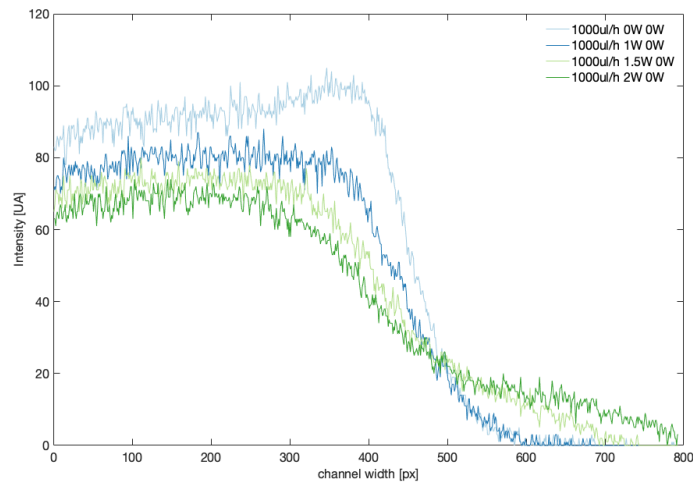


Figure 52: 1000 μ L/h mixing curves, using Violet light

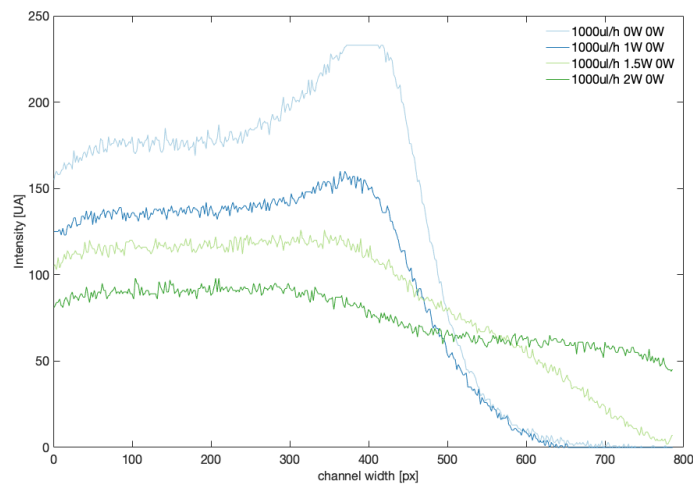


Figure 53: 1000 μ L/h mixing curves, using Green light

As with the curves of 600 and 800 μ L/h, the curve at 2W, in Figure 53, is close to be horizontal, so we can say that it represents high mixing. As we did before, using 70 for 100% mixing and doing a mean for the mixed part, we estimate the mixing percentage. Mean here is 64,03, therefore, the mixing is around 85-90%. The fact that we obtain a higher mixing for 1000 μ L/h than for 800 μ L/h with same power, confirms what we said about the conditions when 2W for 800 μ L/h image was taken, where the mixing should be higher for 800 μ L/h.

- **High flow rates:**

Mixing curves of 2000 μ L/h with maximum power is shown in Figure 54. A displacement in the fluid is noticed, as it can be observed, the intensity in the fluorescent part decreases and some of it goes to the water side, however, not a proper mixing is achieved.

In the future of this project, mixing from below this flow rate to 600 μ L/h will be more detailed studied.

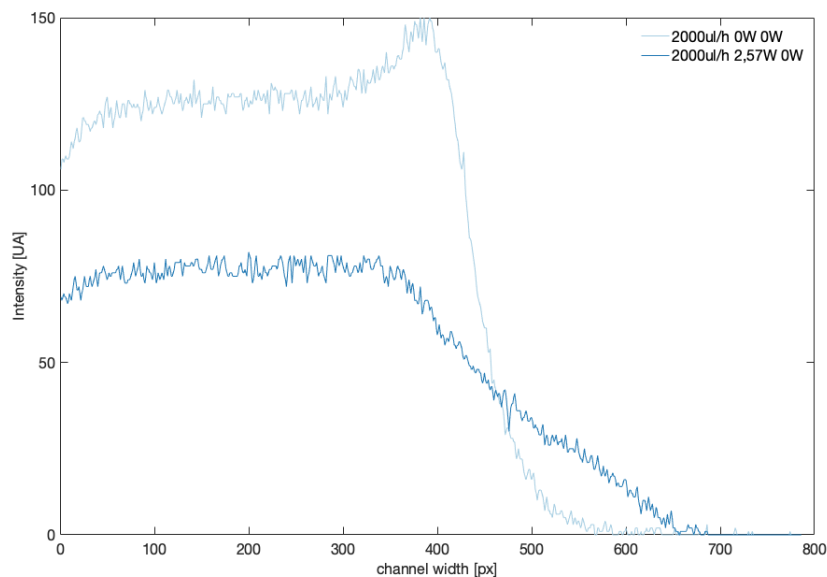


Figure 54: 2000 mixing curves

Mixing for flow rate of 6000 μ L/h will not be plotted, as barely a shift can be observed.

As a summary of this experiment, we could see that when mixing is achieved, the curves tend to the horizontality in the right side of the plot, that corresponds to the microchannel side where water is flowing. We observed that, when a certain power limit is exceeded, mixing starts occurring, so curves tend to horizontality, however, when power is below this limit, there is a curve shift, it is displaced, as the SAW is producing a fluid movement, but it is not enough for breaking the laminar flow.

▪ IDT1 vs. IDT2: Distance study

Next, we will do a result comparison of the mixing produced for IDT1 vs. the mixing produced by IDT2, in order to determine how much the distance to the microchannel matters for mixing.

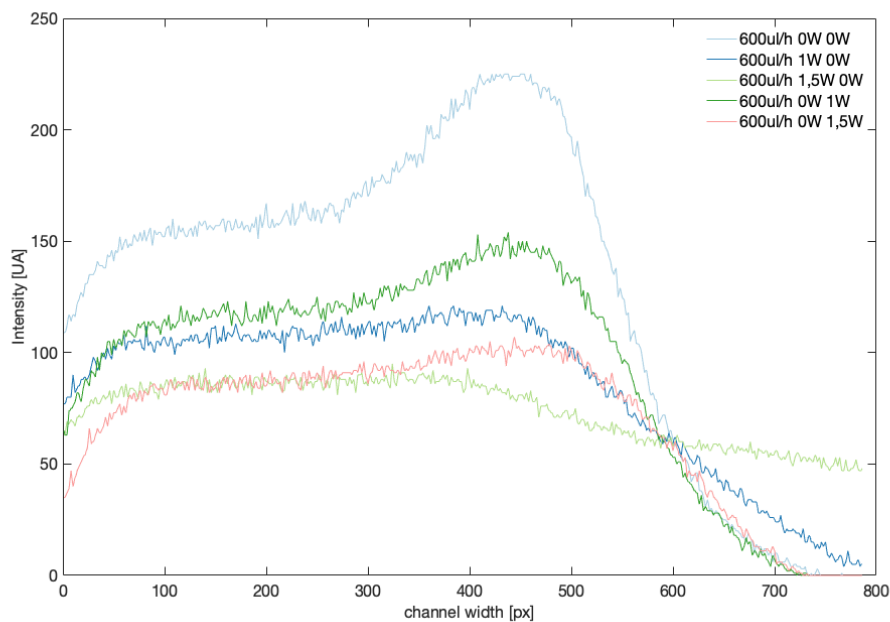


Figure 55: Mixing comparison related to distance to the fluid

In Figure 55, we see how the curves made out of mixing produced on a flow rate of $600\mu\text{L/h}$ by IDT1, compare to the ones made by IDT2, are less sharp on the right side, they tend to horizontality in both sides.

We also can observe that mixing produced by IDT2 is not as uniform as the one IDT1 does, as IDT1 curves tend to horizontality while IDT2's seem to produce a bigger shift in the intensity distribution. This effect looks to be the same as the one produced at low power, instead of mixing it produces a displacement of the fluid inside the microchannel. As IDT2 is placed in the Sulforhodamine B solution side, it is observed that the fluid is displaced towards the centre of the microchannel.

According to the curves, we can appreciate how SAW attenuation affects to mixing, so the closer one allows us to get a higher efficiency.

5.4.2. Dual IDT

Dual IDT performance will be compared with Single IDT's. For this we use images activating both IDT vs. activating only one. Images taken with Violet light.

- **600 μ L/h:**

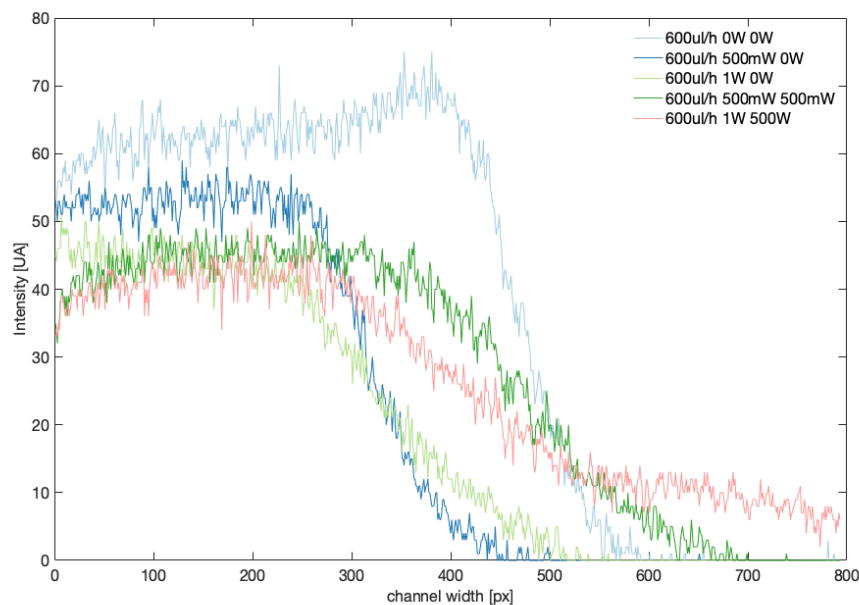


Figure 56: Mixing curves Single IDT vs. Dual IDT for 600 μ L/h

In Figure 56 mixing curves are plotted when one and two IDTs are activated. When only one IDT is activated with 500mW, at this low power what we observe is the fluid displacement explained before. However, when both are activated, even at low power, mixing is achieved. We also can see that is more efficient Dual mixing at 500mW than Single mixing at 1W.

This experiment was done with a light power lower than the others, that's why curves of 500mW and 1W for Single IDT performance here, doesn't correspond with the ones in Figure 47. However, they are enough for the comparison and for getting a conclusion.

- **800 μ L/h:**

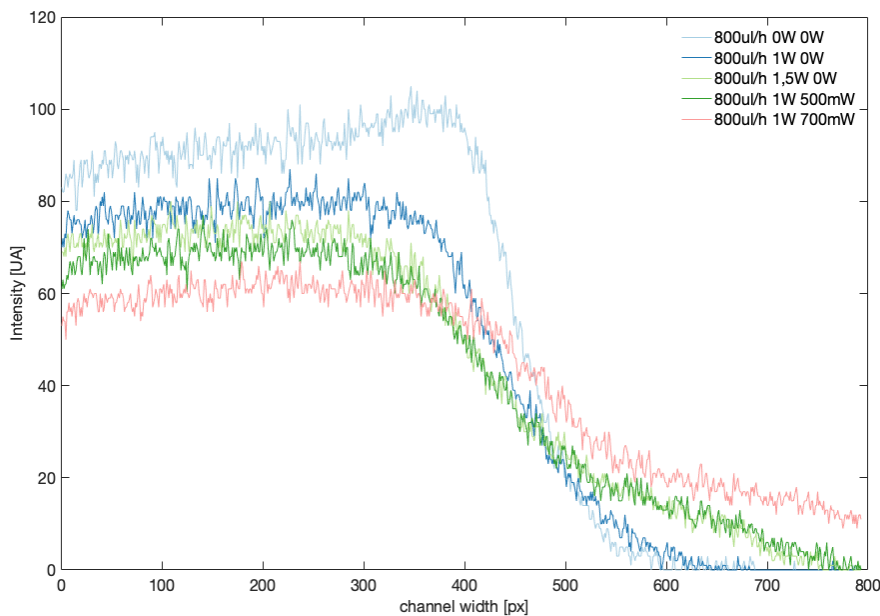


Figure 57: Mixing curves Single IDT vs. Dual IDT performance for 800 μ L/h

Figure 57 represents the mixing curves of mixing of 800 μ L/h, it can be observed that mixing is higher when two IDTs are activated, even using higher power with only one IDT. Curve of 1,5W on IDT with 0W on IDT is slightly lower than curve with 1W with 500mW. Total power is the same, but the performance is better with Dual IDT and

the potential possibilities of this are even higher. As it is shown, mixing with Dual IDT with 1W and 700mW offers the higher efficiency.

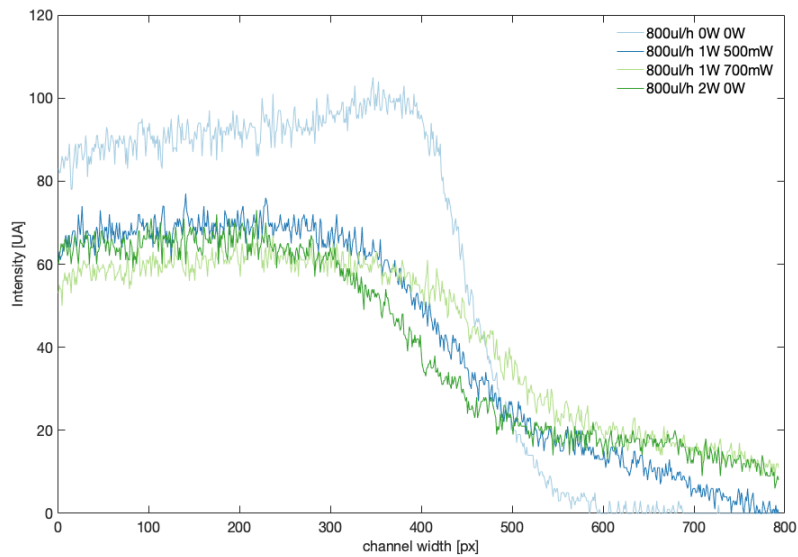


Figure 58: Mixing curve of $800\mu\text{L}/\text{h}$, comparison with maximum power for this flow rate

In Figure 58, mixing using Dual IDT is compared with the higher mixing power possible for this flow rate, we can observe how mixing curve for Dual IDT mixing with 1W and 700mW presents a higher mixing than the Single IDT curve using 2W, a higher total power, because it tends more to horizontality.

Considering Figures 56, 57 and 58, we can affirm that Dual IDT performance is superior compare to Single IDT performance.

If we solve the problem of substrate crash with high powers, we probably could achieve a higher mixing efficiency even for high flow rates.

As a results summary, microfluidics mixing has been studied, identifying its limitations and doing an evaluation of its operational conditions. It has been achieved high efficiency mixing for flow rates between 600 and $1000\mu\text{L}/\text{h}$, comparable results with recent publications, using the smallest microchannel reported in the bibliography and a Single IDT. It also has been studied how the distance between IDT and microchannel affects mixing, due to SAW attenuation. Finally, a comparison between Single and Dual IDT mixing was made, proving that Dual IDT efficiency is higher, however, it exist power limitations for this.

6. Conclusions

The objective of this project was the study of mixing properties of a Surface Acoustic Waves (SAW) mixer. This device was made by the integration of a microchannel with an Interdigital Transducer (IDT), both fabricated using Photolithography.

We achieved high mixing efficiency between flow rates from 600 to 1000 μ L/h, results comparable with recent publications [29], using a Single IDT, with a smaller microchannel than the used in the literature.

Some conclusions obtained from microfluidic mixing study are:

- Single IDT mixing is limited by power apply, which in turn is limited by the appearance of bubbles. Bubbles appearance depends on the flow rate, high flow rates prevent bubbles, but also makes mixing more difficult.
- Dual IDT mixing is limited by the substrate's properties, in a way that Dual IDT performance at high power most likely will produce a substrate crash, ruining the sample.
- Mixing efficiency is highly affected by SAW attenuation, proportional to the distance to the fluid. A closer IDT has a better performance than another further to the fluid
- 80MHz mixers have a higher mixing efficiency than the 120MHz ones.
- Dual IDT mixing have a higher efficiency than Single IDT mixing, into the power limits where Dual IDT performance can operate.

Appendix 1: Fabrication concepts

Maskless aligner:

The steps of the maskless aligner (MLA) process are the same as for regular photolithography with the exception of the exposure, where a mask is no longer needed. The design is introduced as a file in a computer connected to the machine and, instead of subjecting the sample to a flood exposure, the design is directly written using a laser, being unnecessary the use of a mask.

The laser wavelength can be chosen between several options depending of the tool. This kind of exposure allows the user to change the design as many times as wanted, without the need of ordering a mask for a new design. The disadvantages of this tool are its long writing time for complex design, comparing to the time needed for UV lithography. Another disadvantage is that you can't expose several samples at once, as the writing is done sequentially. In this project, an MLA is going to be used, showing the advantages and disadvantages of this tool for patterning in different processes.

PDMS surface activation:

This process is commonly used for cleaning and oxidation of PDMS surfaces, making them hydrophilic, easing aqueous liquids flow through the microchannel and facilitating PDMS bonding. [42]

PDMS oxidation by plasma converts $OSi(CH_3)_2O$ groups, at the surface, into $O_nSi(OH)_{2-n}$, forming covalent siloxane bonds (Si-O-Si). This leads to an irreversible seal of PDMS with a range of materials as itself, glass, silicon, silicon oxide, quartz, silicon nitride and some others. [43]

Lift-off:

Lift-off combined with lithography is a common method for patterning metals e.g. for fabrication of electrodes.

This process is done to remove the pattern written in photolithography, after the metal deposition. Once the lift-off is done, the whole sample remains covered by a metal layer, except for the pattern designed, obtaining the inverse design as, in our case, a gold electrode.



Figure 59: Lift-off representation process.

For this process, it is essential the use of the AZ5214E photoresist, because it allows us to do an image reversal, for guarantying the lift-off. [44]

When you use other kind of photoresist, both positive or negative, the structures obtained after the process form angles below 90° . This makes lift-off more inefficient or even impossible, because gold is also deposited in the sides of the structures, so the acetone is not able to dissolve the photoresist.

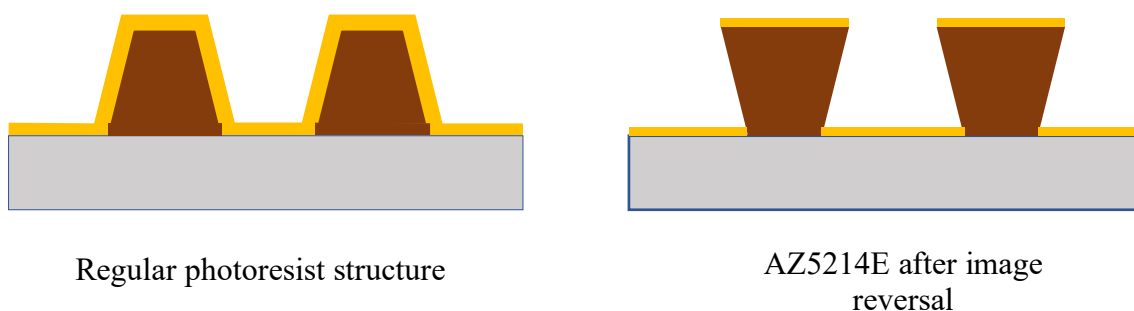


Figure 60: Comparison of gold deposition in a substrate with a photoresist without image reversal vs. AZ5214E

A deposition comparison between a regular photoresist and AZ5214E is shown in Figure 60.

With image reversal, we are able to obtain structures with angles bigger than 90 degrees, so the gold is not deposited on the sides, just in the top of the photoresist. This guaranty the acetone to dissolve the structures, getting a complete and successful lift-off. In Figure 11 we can observe how is the gold deposited over different structures depending of the type of photoresist and the possibility of image reversal.

Appendix 2: Fabrication materials

Substrates:

Silicon wafer:

For microchannel fabrication, we used a 2 inch diameter silicon wafer, provided by NTNU Nanolab with a thickness of 250-300 μm .

LiNbO_3 wafer:

Electric conductive substrate, used for IDT fabrication, provided by NTNU nanolab.

Chemicals:

Cleaning chemicals:

For the wafer cleaning we used two chemicals **IPA** and **Acetone**.

We also used N_2 for drying the sample after cleaning with the chemicals.

Photoresist:

A photoresist is a light-sensitive chemical that we coat the wafer with to obtain the pattern desired, using a light exposure.

During this project we used three different photoresists:

SU-8 3050: It is a negative photoresist used for exposure in the MLA.

DWL 40: It is another negative photoresist used to be exposed in the MLA. It is used in the same process as the SU-8.

AZ5214E: This is a very special photoresist. It is a positive photoresist, and may be used as it, however, it is capable of image reversal and as a result of it, we can obtain a negative pattern. Due of that, AZ5214E can be used as a negative photoresist.

This happen thanks to a special crosslinking agent in the resist formulation which becomes active at temperatures above 110°C and only in the exposed areas. [44]

Developer:

The developer is a chemical used in lithography for the removal of the soluble part of the photoresist after the exposure.

In this project, we used two different developers:

mr-Dev 600: used for development when SU-8 and DWL are used.

AZ726 MIF: used for development when AZ5214E is used.

Machines:

Maskless Aligner (MLA):

The model we use in the Nanolab is the Heidelberg MLA 150.

The MLA150 Maskless aligner is a direct laser write tool, with no need of a mask.

Two laser sources 405nm and 375nm. So all NanoLab photoresists are compatible with the system.

Capable of exposing substrates from 5mm X 5mm up to full 6" wafers or masks.

Substrate thickness must be between 0.1 and 6mm. The system has a topside alignment accuracy of 500nm and backside of 1 μ m. Minimum line width is 1 μ m. The system accepts GDSII, CIF, Gerber and DXF formats. [45]

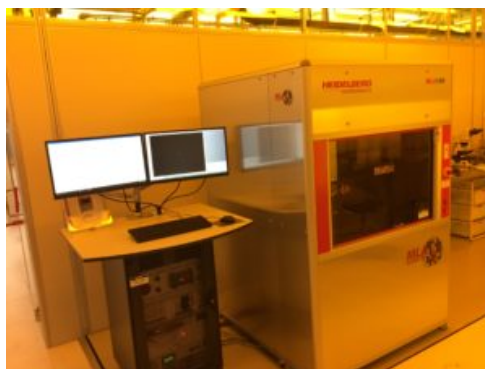


Figure 61: MLA 150 [45]

Plasma Cleaner:

Plasma systems can be used for cleaning and activation of surfaces.

Gas in a low pressure chamber is excited by a supply of energy. Oxygen and ambient air are the gases used in this plasma system. Practically every material can be cleaned with plasma.

The surface is physically cleaned by ion bombardment, and chemically cleaned by the ionized gas. UV radiation helps breaking down long-chain complex carbon compounds. Oxygen plasma creates radical sites on the surface, leaving it hydrophilic.

The maximum generator frequency is 40kHz, maximum flow rate is 200 sccm. [45]



Figure 62: Plasma cleaner

Spin Coater:

The spin coater may be used for coating, etching, cleaning, developing, rinsing/ drying of substrates and coatings but I just used it for coating of photoresist.



Figure 63: Spin coater

AJA sputter and Evaporator:

The AJA Sputter and Evaporator consists of 5 sputter guns and an e-gun with 6 corresponding target pockets.

I used the e-beam evaporator, this can be used to deposit single or multilayer thinfilms of metals, oxides, magnetic materials and dielectrics. An electron beam is swept over the target surface transforming target atoms into gaseous phase which precipitates into solid form coating the chamber. The deposition thickness is controlled by a quartz crystal monitor. The deposition rate is of $5\text{\AA}/\text{s}$. [45]



Figure 64: AJA sputter and evaporator

Mask Aligner MA-6:

It is versatile UV maskaligner that can be used for a wide range of different size samples. It is also capable of doing flood exposures with wavelength filtered to 405nm, 365nm or 320nm. [45]

We will use it for flood exposure for image reversal in the IDT's fabrication process.



Figure 65: MA6 [45]

Wire bonder:

It is a device used to make electrical connections to electronic devices with very thin wires. We use it to connect the IDT to a glass substrate with a gold layer on it, used for testing the IDT's, for this we use gold wires.

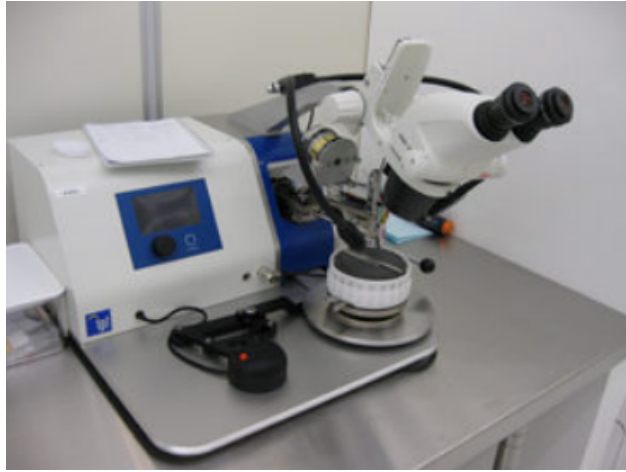


Figure 66: Wire bonder [45]

Appendix 3: Microchannel fabrication process comparison

During the Specialization Project, in order to develop an optimized microchannel fabrication process, we did a comparison between two different photoresist: SU8 and mr-DWL.

Finally we chose SU8, mr-DWL exposition is supposed to be quite faster, but for our design, the process was mostly equal. Also SU8 features were better than mr-DWL ones, shown in Figures 67 and 68.

In Table 3 is explained the time comparison between processes:

Time	SU-8	mr-DWL
Cleaning	8 minutes	8 minutes
Spin coating	3 minutes	3,5 minutes
Soft-baking	15 minutes	12,5 minutes
Exposure	1:50 minutes	50 seconds
Post-exposure baking	5 minutes	12,5 minutes
Development	5 minutes	4 minutes
Total	≈ 38 minutes	≈ 42 minutes

Table 3: Microchannel fabrication process comparison

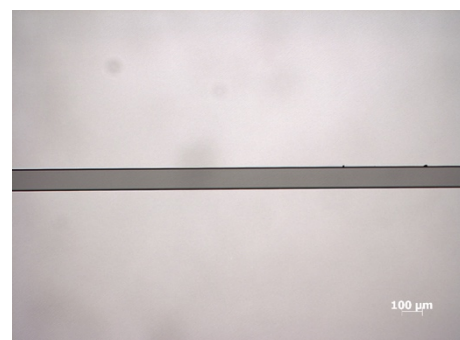
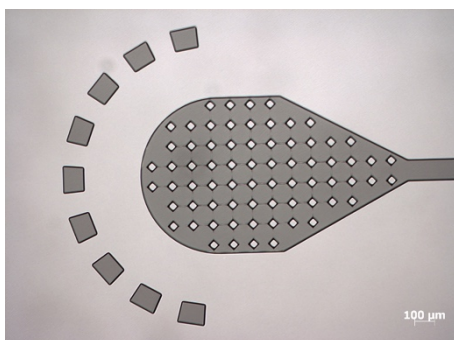


Figure 67: SU8 microchannel pattern features

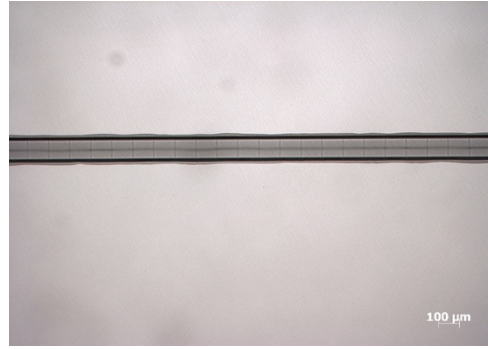
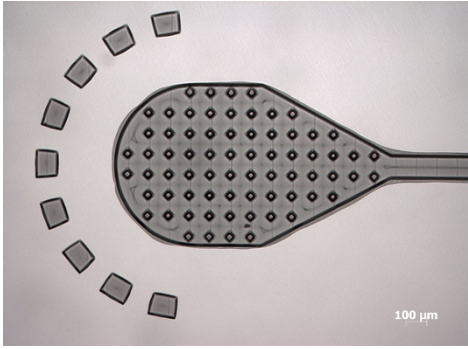


Figure 68: mr-DWL microchannel pattern features

References

- [1] “Exosomes in cancer development, metastasis, and drug resistance: a comprehensive review”; Asfar S. Azmi; Bin Bao; Fazlul H. Sarkar; 2013
- [2] “METAFORA Project - Miniaturised Metabolomics Platform for Microvascular Research - Catching the exosomes”; Yuliya Shakalisava
- [3] “Comparison of ultracentrifugation, density gradient separation, and immunoaffinity capture methods for isolating human colon cancer cell line LIM1863-derived exosomes”; Bow J.Tauro· David W.Greening, Rommel A.Mathias· HongJi· Suresh Mathivanan, Andrew M.Scott, Richard J.Simpson; 2012
- [4] “Microfluidic Systems for Pathogen Sensing: A Review” Jürgen Mairhofer, Kriemhilt Roppert and Peter Ertl; 2009
- [5] “Microfluidic Mixing via Acoustically Driven Chaotic Advection”; Thomas Frommelt, Marcin Kostur, Melanie Wenzel-Schäfer, Peter Talkner, Peter Hänggi, Achim Wixforth ;2008
- [6] “Microfluidic Mixing: A Review”; CY Lee, CL Chang, YN Wang, LM Fu; 2011
- [7] “The origins and the future of microfluidics” George M. Whitesides
Nature volume 442, pages368–373 (2006)
- [8] “Microfluidics: Fluid physics at the nanoliter scale” Todd M. Squires, Stephen R. Quake; 2005
- [9] “Passive mixers in microfluidic systems: A review; Chia-Yen Lee, Wen Teng Wang, Chan-Chiung Liuc, Lung-Ming Fu; 2016
- [10] “A surface acoustic wave (SAW)-enhanced gratingcoupling phase-interrogation surface plasmon resonance (SPR) microfluidic biosensor” A. Sonato, M. Agostini, G. Ruffato, E. Gazzola, D. Liuni, G. Greco, M. Travagliati, M. Cecchini and F. Romanatoad; 2016
- [11] “Waves propagated along” Lord Rayleigh; 1885
- [12] “Direct piezoelectric coupling to surface elastic waves”; R.M. White, F. W. Voltmer; 1965
- [13] “Surface Acoustic Wave Devices and Their Signal Processing Applications”; Colin Campbell; 1989
- [14] “Surface acoustic wave biosensors: a review”; Kerstin Länge, Bastian E. Rapp, Michael Rapp; 2008

- [15] “Microfluidic Mixing via Acoustically Driven Chaotic Advection”; Thomas Frommelt, Marcin Kostur, Melanie Wenzel-Schäfer, Peter Talkner, Peter Hänggi, Achim Wixforth ;2008
- [16] “Study of Surface Acoustic Wave Sensor”; K.Prabakaran1, L.Sujatha; 2017
- [17] “Applications of Surface Acoustic and Shallow Bulk Acoustic Wave Devices” Colin Campbell; 1989
- [18] ”Systems impact of modern Rayleigh wave technology”, Hartman; 1985
- [19] “Interdigital sensors and transducers”; A.V. Mamishev ; K. Sundara-Rajan ; Fumin Yang ; Yanqing Du ; M. Zahn; 2004
- [20] ”Electrical Condenser”; N. Tesla; 1891
- [21] Glassford, A. P. M. J. Vac. Sci. Technol. 1978, 15, 1836-1843.
- [22] Crane, R. A. and Fischer, G. J. Phys. D. 1979, 12, 2019-2026.
- [23] Roederer, J. E.; Bastlaans, G. J. Anal. Chem. 1983, 55, 2333-2336
- [24] “Surface acoustic wave devices as chemical sensors in liquids. Evidence disputing the importance of Rayleigh wave propagation”; Gary S. Calabrese, Hank Wohltjen and Manas K. Roy; 1987
- [25] “Fabrication of an integrated mixing/reaction micro flow cell for μ TAS, Micro Total Analysis Systems '98” , Kluwer Academic Publishers, Dordrecht, 1998, pp. 185–188.; A.Yotsumoto, R.Nakamura, S.Shoji, T.Wada.; 1998
- [26] “Active micro-mixers using surface acoustic waves on Y-cut 128° $LiNbO_3$ ” Wei-Kuo Tseng; 2006
- [27] “High-throughput micromixers based on acoustic streaming induced by surface acoustic wave”; Trung-Dung Luong, Vinh-Nguyen Phan, Nam-Trung Nguyen; 2010
- [28] “Milliseconds mixing in microfluidic channel using focused surface acoustic waves”; Q. Zenga, F. Guoa, L. Yaoa et al.; 2011
- [29] “Dual surface acoustic wave-based active mixing in a microfluidic channel” Myeong Chan Jo, Rasim Guldiken; 2013
- [30] “Micromixing using swirling induced by three-dimensional dual surface acoustic waves (3D-dSAW)”; Jeonghun Nam, Chae Seung Lim; 2017
- [31] “Surface acoustic wave-based micromixing enhancement using a single interdigital transducer”; Husnain Ahmed, Jinsoo Park, Ghulam Destgeer, Muhammad Afzal, and Hyung Jin Sung; 2019

- [32] “The Diamond Ordnance Fuze Laboratory's Photolithographic Approach to Microcircuits”, Jay W. Lathrop; 2013
- [33] “Soft lithography” Younan Xia & George M Whitesides; 1998
- [34] “Manufacturing Techniques for Microfabrication and Nanotechnology”- Chapter 1; Marc J. Madou; 2011
- [35] “Method of making a negative photoresist image”-Patent Holger Moritz Gabor Paal; 1978
- [36] “Conjugate heat transfer analysis of 300-mm bake station”; Natarajan Ramanan, Frank F. Liang, James B. Sims; 1999
- [37] “Soft lithography for micro- and nanoscale patterning”; Dong Qin, Younan Xia & George M Whitesides; 2010
- [38] “Sorption and intraparticle diffusion of fluorescent dyes with consolidated aquifer media”; David A. Sabatini; 2019
- [39] “Continuous particle separation in a microfluidic channel via standing surface acoustic waves (SSAW)”; Jinjie Shi, Hua Huang , Zak Stratton et al.; 2009
- [40] “Versatile platform for performing protocols on a chip utilizing surface acoustic wave (SAW) driven mixing”; Yaqi Zhang, Citsabehsan Devendran et al.; 2019
- [41] “Appl. Phys.”, 112, 084902. M. Alghane, Y. Q. Fu, B. Chen, Y. Li, M. P. Y. Desmulliez and A. Walton, J. 2012
- [42] “Rapid Prototyping of Microfluidic Systems in Poly(dimethylsiloxane)”, David C. Duffy, J. Cooper McDonald, Olivier J. A. Schueller, and George M. Whitesides; 1998
- [43] “Surface molecular property modifications for poly(dimethylsiloxane) (PDMS) based microfluidic devices” Jeong Wong, Chih-Ming Ho; 2009
- [44] “Mechanism and Lithographic Evaluation of image reversal in AZ5214 photoresist”; M. Spak, D. Mammato, S. Jain and D. Durham; 1985
- [45] “Technical Data Sheet AZ5214E”
- [46] NTNU Nanolab webpage

